Outage Analysis and Optimization in Single- and Multiuser Wireless Energy Harvesting Networks

Bo Zhang, Chen Dong, Mohammed El-Hajjar, and Lajos Hanzo

***Abstract*—Compared to battery-powered wireless nodes having a constant but limited power supply, wireless nodes having energy harvesting (EH) capability may greatly prolong the network's sustainability. However, the energy usage policies (EUPs) have to be carefully designed according to the characteristics of the random power supply gleaned from the environment. In this paper, we carry out the outage analysis of a point-to-point (P2P) network relying on an EH transmitter, which has a finite energy buffer (EB) for transmission over a fading channel when having random energy arrival rates. A discrete Markov chain (DMC) model is proposed for characterizing the energy state of the EB, which is then used for quantifying the outage probability (OP) over the fading channels. Then, we propose both a novel 2-D and a low-complexity 1-D search algorithm for finding the specific EUPs, which are capable of minimizing the OP for the P2P network considered. It is shown that the EUP found by both algorithms outperforms the state-of-the-art EUPs disseminated in the open literature. Furthermore, we consider a multiple-access network having M EH-aided sources, where we propose a distributed EUP optimization (DEUPO) algorithm and then minimize the OP relying on the local optimization of each EH-aided source.**

***Index Terms*—Energy harvesting (EH), Markov chain, outage analysis, outage minimization.**

I. Introduction

In practical scenarios such as wireless sensor networks (WSNs), it is challenging to replace the nodes; hence, the network's operation is energy constrained, which is often formulated as having a limited lifetime [1]. One way of circumventing this problem is allowing the nodes to harvest energy from the environment. If a harvested energy source is permanently available, the transceiver can be powered perpetually, which fundamentally changes the wireless system design compared to the classic energy-constrained design relying on an energy source storing a limited amount of energy in batteries. Furthermore, based on the periodicity and magnitude of the harvested energy, the transceiver may adjust its energy usage policy (EUP) to improve certain network performance metrics, such as the throughput or outage probability (OP). The EUP may be defined as the "The policy determining the transmitting power and the transmission rate, given the availability of the knowledge on the amount of energy in the energy buffer, the channel statistic information (CSI) as well as the noncausal energy harvesting information (EHI) characterizing the energy arrival rate at the transmitter."

In this paper, we investigate both the effects of random energy arrival and of the EUP design on the OP of wireless energy harvesting (EH) networks. Recently, the EUP design of EH networks has become a hot research area. Various schemes have been proposed in the literature [2]–[9] to improve certain performance metrics in a particular network topology, relying on different assumptions of the energy arrival rates, as well as on the knowledge available at the wireless transceivers for optimization.

Under the idealized simplifying assumption of having both noncausal channel-state information (CSI) about the CSI to be encountered in the future and about the EH information (EHI) characterizing the energy arrival rate at the transmitter, in [2] and [3],[1] the optimal offline EUPs were designed for point-to-point (P2P) networks using either the throughput maximization or the file-transfer completion-time minimization as the optimization objective function (OF). Later on, the authors in [10] proposed the recursive geometric waterfilling algorithm for solving the same problem, where more efficient recursive computations were used for finding the optimal solutions. In [4], the authors modeled both the uncertainty of the energy arrival rate and that of the data arrival rate, where the transmission rate to be used was determined by minimizing the average data-buffering delay as the OF.

When the instantaneous CSI is not available at the transmitter, having an outage is unavoidable for fixed-rate applications, and the resultant OP of a P2P-EH network was investigated in [5]–[9]. The OP analysis and OP optimization techniques may be categorized into two subclasses according to the knowledge of both the energy arrival rates and the mathematical framework that they adopt; specifically, the first category of contributions recommends the employment of *time-variant policies* [5], [8], [9]. These authors followed the mathematical framework in [2]

Manuscript received December 15, 2014; revised February 19, 2015; accepted February 27, 2015. This work was supported by the Research Councils UK (RC-UK) under the auspices of the India-UK Advanced Technology Center (IU-ATC), by the European Union's Concerto Project, by the European Research Council's Advanced Fellow Grant, and by the Royal Society's Wolfson Research Merit Award. The review of this paper was coordinated by Dr. N.-D. Đào.

B. Zhang is with the School of Electronics and Electrical Engineering, National University of Defense Technology, Changsha 410073, China (e-mail: Bo.Zhang.soton@outlook.com).

C. Dong, M. El-Hajjar, and L. Hanzo are with the School of Electronics and Computer Science, University of Southampton, Southampton SO17 1BJ, U.K. (e-mail: cd2g09@ecs.soton.ac.uk; meh@ecs.soton.ac.uk; lh@ecs.soton.ac.uk).

Color versions of one or more of the figures in this paper are available online at http://ieeexplore.ieee.org.

Digital Object Identifier 10.1109/TVT.2015.2409781

[1] In [2] and [3], the terminology of "transmission policy" was used to represent the policy of using the harvested energy in the energy buffer (EB). However, the transmission policy terminology may be interpreted more widely, such as rate adaptation, multiple-access policy, etc. Therefore, to avoid ambiguity, we use the terminology of "EUP" throughout the paper.

and [11], which adopted the directional waterfilling algorithms under EH-causality constraints[2] for offline EUP design complemented by the stochastic dynamic programming in online EUP design. The time-variant policy implies the fact that the energy usage would be adapted by relying on the idealized simplifying assumptions of having the *a priori* knowledge of the instantaneous energy arrival rates. The second category of EUPs recommends *time-invariant policies for the long transmission durations* routinely encountered in WSNs, which exhibit low computational complexities [6], [7]. The terminology of a time-invariant policy reflects the fact that it does not rely on the idealized knowledge of the instantaneous energy arrival rate, regardless of whether the energy dispensation is designed according to the statistical information of the energy arrival [7] or not [6]. In this case, the EUP may be defined as the "The policy determining the transmitting power, given the amount of energy in the energy buffer and the statistical information of the channel model." *Against this backcloth, in this treatise, we aim for filling the gap between the high-complexity time-variant EUPs and the low-complexity state-of-the-art time-invariant policies, by considering scenarios having a practical finite EB*. As we will show in this paper that the EUPs in the literature [6], [7] did not exploit the EB's state and achieved a suboptimal OP performance. Hence, we propose a range of meritorious methods for improving the OP performance, which fall into the time-invariant category to impose a low computation complexity by relying merely on the knowledge of the average energy arrival rate.

As an evolution of research in the subject area of P2P-EH networks, the recent contributions on EH strategy design also cover multiple-access EH networks [6], [12]–[15]. In [12], Yang and Ulukus investigated the optimal packet scheduling problem in the context of a *two-user fading multiple-access channel*. In [15], Wang *et al.* developed optimal energy scheduling algorithms for a *generalized M-user fading multiple-access channel* relying on EH, to maximize their OF constituted by the network's sum rate, stipulating the idealized simplifying assumption that the side information of both channel states and EH states are known for a certain number of time slots (TSs), where both the battery capacity and the maximum energy consumption during each TS are finite. To the best of our knowledge, the *OP minimization problem of a generalized M-user fading multiple-access channel* is, however, an open problem. Against this background, the novel contributions of this paper are as follows.

1) An analytical framework based on a discrete Markov chain (DMC) is proposed for modeling the EB status, for the sake of investigating the OP of a P2P-EH network, in which an EH source node (EH-SN) equipped with a finite EB transmits to a destination node (DN). Given the EB's size and assuming a certain probability distribution function (PDF) for the energy arrival rate, the OP is derived for arbitrary EUPs.
2) We investigate the optimal EUP conceived for minimizing the OP of a P2P-EH network. Based on our proposed analytical framework, we show that constructing an exhaustive search for finding the optimal EUP for minimizing the OP is impractical, owing to its excessive complexity, because it scales with $(L_{\max})!$, where $L_{\max}$ is the number of states in the DMC. Therefore, a heuristic 2-D search (2D-search) algorithm is proposed for finding a meritorious EUP; we demonstrate that the proposed algorithm is potentially capable of finding the EUP at a manageable complexity.[3]
3) Nonetheless, the 2D-search algorithm conceived still exhibits a high complexity; hence, we also propose a low-complexity 1-D search (1D-search) algorithm. We will demonstrate that the OP of the 1D-search algorithm is close to that of its 2D-search counterpart, which may be attractive for applications relying on low-cost hardware, such as mobile phones and wireless sensors.
4) We extend the proposed DMC framework to more general nonorthogonal EH networks. In contrast to the P2P scenario, the outage events of practical EH-SNs tend to be correlated. As an attractive application scenario, we will investigate the OP of maximum-likelihood (ML) detection in the context of spatial-division multiple-access (SDMA) networks, we will decompose the OP by approximating it as multiple independent outage probabilities, each corresponding to a simple P2P-EH-network subproblem. Finally, we will propose a distributed EUP optimization (DEUPO) protocol, where each EH-SN is capable of optimizing its own policy using both the local statistics of the fading channel and the related energy arrival model.

The rest of this paper is organized as follows: In Section II, we first discuss the EUPs found in the literature and then invoke the DMC for modeling the EB's state. Based on this model, we consider the OP minimization problem and propose the aforementioned 2D-search and 1D-search algorithms conceived for finding the optimal EUPs. In Section III, we investigate the EUP design of SDMA-EH networks, and we propose the aforementioned distributed DEUPO protocol. Finally, our conclusions are presented in Section V.

II. Peer-To-Peer–Energy Harvesting Network Design

A. System Model and OP Formulation

We first consider a simple P2P network constituted by an SN and a DN, which is shown in Fig. 1. As shown in Fig. 1,

[2]The EH-causality constraint refers to the fact that, at any time, the transceivers can only utilize the energy that was harvested during the past and the energy not harvested as yet is hence unavailable for usage. Taking into account the causality constraints imposed on the energy usage, the energy can only be saved and used in the future. Therefore, the waterfilling algorithm is redesigned as a directional one, which allows the energy flow only to take place from the past to the future.

[3]When the Markov chain model has $L_{\max} \leq 10$ states and the number of OF evaluations is lower than 10!, the exhaustive searching may be implemented and therefore may serve as the benchmark for our proposed algorithm. However, for $L_{\max} > 10$, the complexity becomes excessive, which prevents us from verifying, whether the 2D-search algorithm is capable of matching the optimal EUP. On the other hand, it is challenging to mathematically prove the optimality of a search algorithm in the context of a nonconvex problem involving high-dimensional matrices. Therefore, this open problem will be further detailed in our discussions, and it will be investigated in our future work.

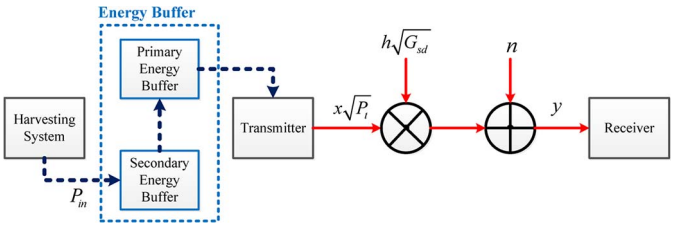

Fig. 1. System model of the P2P-EH network.

a primary EB and a secondary EB is required in practice [1], [6]. In [1], the secondary storage is a backup storage invoked for situations, when the primary storage is exhausted. In [6], the authors assumed that the rechargeable energy storage devices cannot charge and discharge simultaneously; hence, the transmitter is powered by the primary EB for data transmission, while the secondary EB is connected to the harvesting system and charges up. At the end of the recharge cycle, the secondary EB would be charged by the secondary EB. We assume that the charging time of the primary EB is negligible[4] and that the charging efficiency is assumed to be 100%.[5] Therefore, both the primary and the secondary EBs may be represented by a single EB, which is represented by the dashed-line box shown in Fig. 1. This buffer is assumed to be capable of powering the transmitter, while simultaneously being charged by the harvesting system. We do not make any specific assumptions as to what harvesting system is adopted, which may be solar cells, a wind anemometer, etc., as discussed in [1]. We assume that the EB at the SN has a finite EB size, where the harvested energy is stored and used for transmission. We assume furthermore that the energy arrival rate $P_{\rm in}$ obeys a certain probability distribution with an expectation of $\overline{P}_{\rm in}$, and it remains constant over a TS of duration T_E, while changing independently over the subsequent TSs, where a time slot is a recharge cycle. We assume that the instantaneous energy arrival rate is unknown and cannot be used during the current TS of T_E, because the secondary EB is not allowed to charge and discharge simultaneously, as shown in Fig. 1. In order to focus our attention on the EUP conceived for wireless transmission, we assume that the circuit power consumption at the SN is negligible and that the energy conversion efficiency between the EB and the transmit power is 100%.[6]

Let us now consider the channel modeling of the wireless communication links. We consider a narrow-band block-fading channel model, where the fading coefficients remain constant for the duration of a transmission packet denoted by T_C and then they are faded independently from one packet to another over the time dimension. Note that we make no assumptions concerning the specific channel model and the distribution of the channel gain. We also assume that there are always data packets buffered at the SN for transmission. The signal received at the DN is represented by

$$y = h\sqrt{P_t}G_{sd}x + n \tag{1}$$

where h is the channel coefficient capturing the effects of fading, while P_t is the transmit power, x is the transmitted signal, and n is the additive noise at the receiver, which is modeled by independent standard circularly symmetric complex Gaussian random variables having a zero mean and a variance of 1. In (1), the average processing gain of $G_{sd} = \left(N_0 \times d_{sd}^{\beta}\right)^{-1}$ between the SN and the DN captures the effect of both the pathloss and the noise, where N_0 is the noise power at the receiver, d_{sd} is the distance between the SN and the DN, while β is the pathloss exponent.

An outage is defined as the event when the instantaneous received signal-to-noise power ratio (SNR) γ at the receiver is below a predefined threshold $\gamma_{\rm th}$ that has to be exceeded for successful decoding. If idealized perfect capacity-achieving coding is assumed, we have $\gamma_{\rm th} = 2^R - 1$, where R is the data transmission rate [16]. Then, the OP of the single-hop EH network may be expressed as follows:

$$\begin{aligned} P_{\rm out} &= \Pr\left\{P_t|h|^2 G_{sd} < \gamma_{\rm th}\right\} \\ &\triangleq \Pr\left\{P_t|h|^2 < P_{\rm th}\right\} \end{aligned} \tag{2}$$

where P_t is the transmit power, and h is the normalized channel coefficient capturing the fading effects. In (2), we define $P_{\rm th} = \gamma_{\rm th}/G_{sd}$, to focus our attention on the effects of both the transmit power P_t and the channel's fading coefficient h.

In the conventional transmission scheme relying on classic constant power supply, the transmit power P_t is a constant, and the corresponding OP of narrow-band block-fading channels was quantified in [16]. However, in the EH networks, the instantaneous transmit power P_t is time variant, which is constrained by the amount of the energy available in the EB, which in turn is a random variable depending on the energy arrival rate. The energy arrival rate is assumed to exhibit a blockwise fluctuating nature, which remains constant over a TS of duration T_E and changes independently over the subsequent TSs. During a TS with a duration of T_E, the amount of energy harvested, i.e., $P_{\rm in}T_E$, is independent of both that harvested in the previous TS and of the energy consumed, i.e., P_tT_E, during transmission, which is determined by the EB state B_T at the beginning of the current TS.

We define the EB state as $B_T = B_E/T_E$, where B_E is the amount of energy available in the EB, while T_E is the duration of the recharge cycle. The physical interpretation of B_T is the maximum average transmit power that may be supported by the amount of energy stored in the buffer during the current recharge cycle.[7] *The EH-causality constraint* [2] *is interpreted*

[4]In practice, this may be realized by a supercapacitor-based storage system, such as, for example, the Everlast solar system introduced in [1].

[5]In practice, the charging efficiency of the secondary EB may not reach 100%; hence, it may be multiplied by an efficiency factor $\eta_{\rm buffer} \in [0, 1]$, which may be equivalently considered to be a reduced energy arrival rate, and hence, it does not affect any of our analysis.

[6]In practice, the power consumption of the circuits may be nonnegligible. We may assume that the harvesting system is capable of providing sufficient circuit power, while additionally providing a nonnegative transmit power. When the EH system is not capable of supplying sufficient circuit power, the transmitter may be switched off. On the other hand, the energy conversion efficiency $\eta_{\rm TX}$ from the EB to the transmitter cannot reach 100% in practice. Hence, we may simply multiply the energy arrival rate at the transmitter with an efficiency coefficient $\eta_{\rm TX} \in [0, 1]$, which does not affect any of our analysis.

[7]When the knowledge of the instantaneous CSI during a period is unavailable at the transmitter, transmitting at a constant transmit power would achieve the minimum OP [16]. Therefore, a constant transmit power is adopted during each recharge cycle, and B_T is the upper bound.

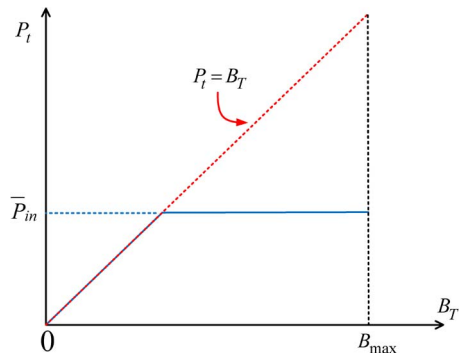

Fig. 2. EUP illustrated as the function of P_t versus B_T.

as follows: the instantaneous transmit power P_t cannot exceed the maximum power B_T that may be supported by the current EB state, i.e., we have $P_t \leq B_T$, explicitly indicating that the energy assigned for transmission must not exceed the amount of energy harvested. We may model the EUP by the transmit power as a function of the EB state, as follows:

$$P_t(B_t),\ B_T \in [0, B_{\max}] \tag{3}$$

where the EB state B_T is upper bound by $B_{\max}$ defined as the EB capacity divided by the recharge cycle T_E.

In Fig. 2, the EH-causality constraint is shown in dashed lines as $P_t(B_T) = B_T$, which models the best-effort policy proposed in [6], where all harvested energy in the buffer is used up for transmission. On the other hand, the asymptotic optimal policy proposed in [7] is illustrated by the solid line in Fig. 2, where the SN aims to transmit at a power of $P_t = \overline{P}_{\text{in}}$. In the asymptotic optimal policy, when the remaining energy in the EB is capable of supporting a higher transmit power than the average energy arrival rate $\overline{P}_{\text{in}}$, the transmitter conserves the energy for its future usage. If the remaining energy in the EB is insufficient for supporting $P_t = \overline{P}_{\text{in}}$, the SN switches to the best-effort policy. We may formulate the OP of the P2P-EH network as follows:

$$\begin{aligned} P_{\text{out}}(P_t) &= \int_0^{B_{\max}} \Pr\left\{P_t(x)|h|^2 < P_{\text{th}}\right\} f_{B_T}(x)dx \\ &= \int_0^{B_{\max}} \int_0^{+\infty} \Pr\left\{P_t(x)y < P_{\text{th}}\right\} f_{|h|^2}(y) f_{B_T}(x)dx \end{aligned} \tag{4}$$

where h is the channel coefficient capturing the effects of fading, which is a random variable, and its PDF $f_{|h|^2}(y)$ relies on the statistical channel model. $f_{B_T}(x)$, $x \in [0, B_{\max}]$ is the PDF of the EB state B_T. Therefore, to derive the OP formulated in (4), the PDF of the EB state B_T has to be modeled, bearing in mind the specific EUP adopted. Furthermore, because both P_t and B_T are continuous variables, the number of feasible EUPs is infinite, and since different policies would result in different EB-state PDFs, finding the optimal policy for minimizing the OP in (4) may be quite challenging. Hence, we will investigate this problem in the next section.

B. DMC Modeling of the EB State

As the energy arrival rate P_{in} is assumed to be constant over a recharge cycle T_E and then changes independently over the subsequent recharge cycles, the EB state $B_T(k)$ at the end of the kth $(k \geq 1)$ recharge cycle relies only on the state of $B_T(k-1)$, on the amount of energy consumed for transmission $P_t[B_T(k)]$, as well as on the current energy arrival rate P_{in}, which obeys a certain PDF, but it is statistically independent of its previous samples. Therefore, B_T may be modeled by a continuous Markov process.

However, the domain of $B_T \in [0, B_{\max}]$ is continuous; hence, the set of the states is uncountable and challenging to manage [17]. Therefore, given the EUP, deriving the PDF of B_T is quite challenging, except for certain special cases, such as the best-effort policy combined with the condition, when the transmit power is equal to the instantaneous arriving energy, which may be modeled by the exponential distribution [6]. Even for the asymptotic optimal policy [7], where P_t is a simple function determined by a combination of the best-effort policy and of the constant power supply, the PDF of B_T cannot be readily derived in closed form; hence, the asymptotic optimality relies on the fact that the probability of $\Pr\{B_T < P_t = \overline{P}_{\text{in}}\} \to 0$, when the EB size obeys $B_{\max} \to \infty$. In order to quantify and then to minimize the OP in (4), we approximate the continuous-state Markov process by a finite-state Markov chain [18], to model the EB state B_T, and to derive the PDF of B_T. Specifically, the EB size $B_{\max}$ is discretized as $L_{\max} = \lfloor B_{\max}/\varepsilon_P \rfloor$, where ε_P is the discrete step size of the power. Therefore, $l = \lfloor B_T/\varepsilon_P \rfloor$ may take a value from $l \in \{0, 1, \ldots, L_{\max}\}$ and has a state-space size of $(L_{\max} + 1)$. The instantaneous EH rate P_{in} and the decoding threshold P_{th} are also discretized with a step size of ε_P as

$$\begin{aligned} L_{\text{in}} &= \left\lfloor \frac{P_{\text{in}}}{\varepsilon_P} \right\rfloor \\ L_{\text{th}} &= \left\lfloor \frac{P_{\text{th}}}{\varepsilon_P} \right\rfloor. \end{aligned} \tag{5}$$

Hence, L_{th} is a discrete constant when P_{th} is given, while l and L_{in} are discrete random variables, and their probability mass functions (PMFs) may be generated from the PDFs of B_T and P_{in} as follows:

$$\begin{aligned} \Pr\{l = x\} &= \int_{x\varepsilon_P}^{(x+1)\varepsilon_P} f_{B_T}(u)du \\ \Pr\{L_{\text{in}} = x\} &= \int_{x\varepsilon_P}^{(x+1)\varepsilon_P} f_{P_{\text{in}}}(u)du. \end{aligned} \tag{6}$$

Although the variables B_T, P_{in}, and P_t may assume any arbitrary continuous nonnegative value, the DMC may be capable of sufficiently accurately capturing the buffer's behavior, as long as the discretization step size ε_P is small enough. Finally, we may discretize the EUP formulated in (3) as

$$P_t(l) = P_t\left(\left\lfloor \frac{B_T}{\varepsilon_P} \right\rfloor\right),\ l \in \{0, 1, \ldots, L_{\max}\} \tag{7}$$

where the discrete EUP is defined as

$$L_t(l) = \left\lfloor \frac{P_t(l)}{\varepsilon_P} \right\rfloor. \tag{8}$$

Then, we may construct the state transition matrix T of the EB states, where the specific element in the ith row and jth column is given by

$$\begin{aligned} T_{i,j} &= \Pr\{l(k+1) = j \mid l(k) = i\} \\ &= \begin{cases} \Pr\{j = i + L_{\text{in}} - L_t(i)\}, & 0 \le j < L_{\max} \\ \Pr\{j \le i + L_{\text{in}} - L_t(i)\}, & j = L_{\max}. \end{cases} \end{aligned} \tag{9}$$

We arrive at the steady-state probability vector $\pi = [\pi_0\ \pi_1\ \ldots\ \pi_{L_{\max}}]^T$ using the relationship of

$$\pi = T^T \pi \tag{10}$$

where the physical interpretation of (10) is that the state probability vector π converges and remains constant. Then, we may formulate the OP as

$$\begin{aligned} P_{\text{out}}\left(L_t(l)\right) &= \sum_{l=0}^{L_{\max}} \Pr\left\{L_t(l)|h|^2 < L_{\text{th}}\right\} \pi(l) \\ &\triangleq \sum_{l=0}^{L_{\max}} P_e(l)\pi(l) \end{aligned} \tag{11}$$

which is the discrete version of (4). It should be noted that, in (11), the OP component of $P_e(l) \triangleq \Pr\{L_t(l)|h|^2 < L_{\text{th}}\}$ is not determined unambiguously by the EUP defined by $L_t(l)$, $l \in [0, L_{\max}]$, because it also relies on the statistical channel model determining the distribution of $|h|^2$. For example, if a narrow-band Rayleigh block-fading channel is assumed, then $|h|^2$ follows the exponential distribution in conjunction with the parameter of 1. In this case, the OP component $P_e(l)$ may be expressed as

$$P_e(l) = \Pr\left\{L_t(l)|h|^2 < L_{\text{th}}\right\} = 1 - e^{-\frac{L_{\text{th}}}{L_t(l)}}. \tag{12}$$

C. Two-Dimensional EUP-Search Algorithm

Given a certain EUP represented by $L_t(l)$, $l \in [0, L_{\max}]$ and a specific statistical channel model, we are now capable of quantifying the OP of a certain EUP with the aid of (7)–(11). The optimal EUP $L_t(l)$, $l \in [0, L_{\max}]$ may be formulated by using the physically meaningful OF minimizing the OP as follows:

$$\min_{L_t(l)}\ P_{\text{out}}\left[L_t(l)\right]. \tag{13}$$

However, the inverse of the mapping in (11) from the OP $P_{\text{out}}[L_t(l)]$ to the specific EUP $L_t(l)$ cannot be readily evaluated. In other words, given a certain $P_{\text{out}}[L(l)]$, it is not possible to derive the EUP $L_t(l)$ adopted. Naturally, this hinders the related inverse mapping, and hence, the closed-form derivation of the optimal EUP is not possible. Although the buffer-state transition matrix T of (9) may be readily determined, given the EUP $L_t(l)$, according to (9), the resultant steady-state probability vector $\pi = [\pi_0\ \pi_1\ \ldots\ \pi_{L_{\max}}]^T$ is a solution of (10), which is a high-dimensional system of linear equations. Furthermore, given a certain steady-state probability vector π, it is not possible to derive the buffer-state transition matrix T, and hence, we cannot uniquely and unambiguously determine the discrete EUP $L_t(l)$.

1) Design Motivations: When using a discrete Markov modeling of the EB state, the EUP is represented by a vector of $L_t(l), l \in [0, L_{\max}]$, which has $(L_{\max}+1)$ legitimate elements over the first dimension constituted by the EB state, where the lth element in $L_t(l)$ itself may be assigned any discrete value spanning from 0 to l over the second dimension representing the amount of energy assigned for transmissions. Hence, the EUP search is over a 2-D space. The aforementioned fact motivates us to design an EUP-search algorithm. The most conceptually straightforward way of finding the optimal EUP $L_t(l)$, $l \in [0, L_{\max}]$ is to invoke an exhaustive search, which evaluates every feasible EUP and selects the one having the minimum OP. As illustrated in Fig. 2, an EUP $L_t(l)$ is physically feasible as long as the instantaneous transmit power P_t is nonnegative and does not exceed the maximum affordable power B_T that may be supported by the current EB state $P_t \le B_T$, which is equivalent to the following discrete form:

$$0 \le L_t(l) \le l,\ \forall l \in [0, L_{\max}]. \tag{14}$$

This simple feasibility constraint results in a large number of feasible EUPs, where the complexity of searching for the optimal policy that minimizes the OP may be excessive. Quantitatively, there are $N_f = (L_{\max}+1)!$ number of feasible functions of $L_t(l)$, given the condition in (14). For example, if we have $L_{\max} > 11$, the number of feasible functions becomes $N_f > 10^8$. Therefore, the exhaustive search method of finding the optimal policy is not practically feasible. Hence, we have to design search algorithms having a practically tolerable complexity, which are detailed in the following sections.

2) EUP-Search Algorithm Design: In the algorithms proposed in this treatise, the design guidelines that we adopted for controlling the complexity, which is quantified by *the number of OP evaluations*, are summarized as follows.

- **Guideline 1**: *The optimal EUP $L_t(l)$, $l \in [0, L_{\max}]$ is a nondecreasing function of the EB state l, i.e., we have* $\forall k \in [0, L_{\max}-1]$, $L_t(k+1) - L_t(k) \ge 0$. The physical interpretation of this guideline can be summarized as follows. If the amount of energy available in the EB is increased, the transmitter should not use a lower transmit power. The reason behind this guideline is twofold: First, the transmitter has no knowledge of the energy arrival rate in the future; therefore; it cannot decide as to whether conserving the harvested energy in the EB for future usage is beneficial. Second, the transmitter has no knowledge of the instantaneous channel gain; therefore, it cannot decide how to control the transmit power.

- **Guideline 2**: *The increment of the optimal EUP* $L_t(l)$, $l \in [0, L_{\max}]$ *is no higher than one unit of energy with respect to the EB state* l, *i.e., we have* $\forall k \in [0, L_{\max}-1]$, $L_t(k+1) - L_t(k) \leq 1$. Let us assume that there are two feasible EUPs L_t and $\hat{L}_t$, which satisfy $L_t(k+1) - L_t(k) \geq 2$, $\hat{L}_t(k+1) - \hat{L}_t(k) \leq 1$, and $\hat{L}_t(k+1) + \hat{L}_t(k) = L_t(k+1) + L_t(k)$. When the OP versus the transmit power is a convex function, the algorithm should choose $\hat{L}_t$, because according to (11), it would achieve a lower OP than L_t, provided that the steady-state probability vector π is assumed to be fixed. However, it was shown in [8] that the OP functions with respect to the transmit power are nonconvex in the low transmit power region, i.e., when $P_{\text{out}} > 0.1$. However, in most practical scenarios, a better OP is required, in which case the OP functions tend to be convex. In this scenario, evenly allocating the transmit power to state k and $(k+1)$ may achieve a lower OP than an unequal allocation of power, given a fixed total amount of transmit power. Therefore, we judiciously opt for EUPs satisfying $L_t(k+1) - L_t(k) \leq 1$.

Although the aforementioned pair of design guidelines may be interpreted physically in a simple manner, it is challenging to rigorously prove the optimality of *Guideline 1*, while *Guideline 2* is applied in a relatively high transmit power scenario associated with a good channel quality, when the OP is a convex function of the transmit power [8]. When relying on the proposed pair of design guidelines, the number of OP evaluations is reduced from $N_f = (L_{\max})!$ to $N_{2D} = 2^{N_{\max}}$, which may still be excessive. Quantitatively, when we have $N_{\max} > 30$, the number of OF evaluations obeys $N_{2D} > 10^9$. Therefore, we conceive a third guideline for controlling the complexity, albeit this is achieved at the cost of potentially resulting in a locally optimal solution, which is detailed as follows.

- **Guideline 3**: *When the search does not find an EUP resulting in a reduced OP, it is terminated*. This is a widely used early-stopping technique employed in heuristic optimization algorithms [19]. Albeit its global optimality is not guaranteed without further information about the search space, it is capable of substantially reducing the complexity.

Since *Guideline 3* may result in locally optimal solutions, multiple initial solutions may be chosen for the search algorithm. However, through our extensive numerical evaluations conducted for $N_{\max} < 12$, when the exhaustive search algorithm is still feasible, our numerical results have shown that Algorithm 1 is capable of finding the globally optimal EUP. Algorithm 1 uses the best-effort policy as the initial solution, and then, the three aforementioned guidelines are followed throughout the rest of the design. Therefore, it may be concluded that, although the optimality may not be shown mathematically, the proposed heuristic 2D-search algorithms are effective in practical applications, while imposing a much lower complexity than the exhaustive search.

Algorithm 1 2D-Search Algorithm

$L_t(l) = l, l \in [0, L_{\max}]$;**//Start as the best-effort policy**
$P_{\text{out,min}} \leftarrow 1$;
$N_I \leftarrow 0$;
$I_U \leftarrow 1$;
while $I_U == 1$ **do**
  $N_I \leftarrow N_I + 1$; //record the number of searches
  for $l = L_{\max}$ to 0 **do**
    $\widetilde{L}_t \leftarrow L_t$; //store the current policy
    if $L_t(l) > 0$ **then**
      $L_t(l) \leftarrow L_t(l) - 1$; **//remove the top tile only (guideline 2)**.
    end if
    for $i = 0$ to l **do**
      $L_t(i) \leftarrow \min(L_t(i), L_t(l))$; **//ensure policy is non-decreasing (guideline 1)**.
    end for
    $P_{\text{out}} = P_{\text{out}}(L_t)$;
    if $P_{\text{out}} < P_{\text{out,min}}$ **then**
      $P_{\text{out,min}} \leftarrow P_{\text{out}}$;
    else
      $L_t \leftarrow \widetilde{L}_t$; //recover the stored policy
    end if
    $L_t[N_I] \leftarrow L_t$;
    if $L_t[N_I] == L_t[N_I - 1]$ **then**
      $I_U \leftarrow 0$; **//terminate if the iteration (guideline 3)**.
    end if
  end for
end while

D. One-Dimensional EUP-Search Algorithm

In the previous section, the optimal EUP was investigated and a 2D-search algorithm was proposed. However, the algorithm relies on searching in a 2-D domain of the EB state and of the energy assigned for transmission; hence, it is quite involved. Here, motivated by the fact that the asymptotic optimal policy is characterized by a constant desired transmit power [7], we formulate a 1D-search-based EUP and aim for minimizing the OP using a reduced-complexity 1-D search to exhibit a significantly lower complexity than that of the 2D-search algorithm.

1) Design Motivations: Our proposed 1D-search policy is motivated by the asymptotic optimal policy proposed in [7], which is illustrated in Fig. 2. The suboptimal EUP considered is based on a combination of the constant power policy and the best-effort policy. Specifically, given a desired constant transmit power P_d, when the energy remaining in the EB satisfies $B_t \geq P_d$, the transmitter opts for transmitting at a power of $P_t = P_d$ and conserves the rest of the energy for its future usage. Otherwise, when $B_t < P_d$, the transmitter switches to the best-effort policy and transmits at a power of $P_t = B_T$. The suboptimal policy is represented by a fixed $P_t(B_T)$ of

$$P_t(B_T) = \begin{cases} B_T, & B_T < P_d \\ P_d, & B_T \geq P_d \end{cases} \tag{15}$$

while its discrete version represented by $L_t(l)$, $l \in [0, L_{\max}]$ is

$$L_t(l) = \begin{cases} l, & l < L_d \\ L_d, & l \geq L_d \end{cases} \tag{16}$$

where we define $L_d = \lfloor P_d/\varepsilon_P \rfloor$. Compared to the generalized representation of $L_t(l)$, $l \in [0, L_{\max}]$, which requires $(L_{\max} + 1)$ variables for fully characterizing the policy, the proposed EUP may be characterized by a single variable L_d. Therefore, L_d is also the only variable that may be optimized to minimize the OP. However, the 1D-search policy may be expected to result in a degraded OP.

A special case of the proposed EUP is to set $P_d = \overline{P}_{\text{in}}$ or equivalently $L_d = \overline{L}_{\text{in}}$. The asymptotic optimal EUP proposed in [7] was shown to achieve the performance of its constant-power counterpart operating at $P_t = \overline{P}_{\text{in}}$, based on the assumption of an infinite EB size of $B_{\max} \to \infty$ [7]. In this case, the probability of an EB overflow is 0, and the probability of $\Pr\{B_T < P_d\} = \Pr\{l < L_d\} \to 0$. It is plausible that the performance of the classic non-EH system constitutes the OP lower bound that may be achieved by any EH system relying on a random energy arrival rate. Naturally, achieving the performance of the asymptotic optimal EUP is desirable [7].

However, when the EB size is finite, the asymptotic optimal policy would be suboptimal, because a finite EB may overflow with a nonnegligible probability, when the instantaneous energy arrival rate is high and cannot be stored for future usage. Meanwhile, the choice of $L_d = \overline{L}_{\text{in}}$ may not be optimal, since a choice of $L_d \neq \overline{L}_{\text{in}}$ may reduce both the probability of EB overflow and the OP. However, the optimal choice[8] of P_d is not obvious, because the relationship between the OP P_{out} and the energy usage function L_t is quantified by (9)–(11), which makes the direct derivation of the optimal P_d quite challenging.

By comparison, as shown in (7)–(11), given a specific value of P_d, the numerical evaluation of P_{out} may be straightforward, according to the OP expression provided in (11). This motivates us to design a search algorithm, which searches for the optimal P_d based on the numerical evaluation of P_{out}, instead of using an analytical derivation to get the optimal P_d directly.

In the next section, we will first derive the OP for the 1D-search-based EUP given a specific L_d and then propose our specific search algorithm for finding the optimal L_d to minimize the OP.

2) One-Dimensional EUP-Search Algorithm Design: Upon invoking the 1D-search-based EUP represented in (16), we may simplify the OP expression of (11) specifically for the 1D-search policy as follows:

$$\begin{aligned} P_{\text{out}} = {} & \Pr\{l \geq L_d\} \Pr\left\{L_d|h|^2 < L_{\text{th}}\right\} \\ & + \Pr\{l < L_d\} \Pr\left\{l|h|^2 < L_{\text{th}} | l < L_d\right\} \end{aligned} \tag{17}$$

where the first line represents the OP, when the energy in the EB is capable of supporting transmitting at the desired level of L_d. The second line in (17) represents the OP, when the energy in the EB is insufficient for transmitting at the power level of $L_t = L_d$, and the transmitter consumes all the energy in the EB, while transmitting at a power level of $L_t = l$. Then, we construct the state transition matrix T of the EB state according to (9), and when the EB state is steady, the state probability vector π may be formulated as follows:

$$\pi = T^T \pi$$

where $\pi = [\pi_0 \ \pi_1 \ \ldots \ \pi_{L_{\max}}]^T$. Given the desired power level represented by L_d and the OP expression in (17), we have

$$\Pr\{l \geq L_d\} = \sum_{l=L_d}^{L_{\max}} \pi_l. \tag{18}$$

If we assume furthermore that the channel obeys Rayleigh fading, the other terms in (17) can be derived as follows:

$$\Pr\left\{L_d|h|^2 < L_{\text{th}}\right\} = 1 - \exp\left(-\frac{L_{\text{th}}}{L_d}\right) \tag{19}$$

$$\begin{aligned} & \Pr\{l < L_d\} \Pr\left\{l|h|^2 < L_{\text{th}} | l < L_d\right\} \\ & = \sum_{l=0}^{L_d-1} \pi_l \Pr\left\{l|h|^2 < L_{\text{th}}\right\} \\ & = \sum_{l=0}^{L_d-1} \pi_l \left[1 - \exp\left(-\frac{L_{\text{th}}}{l}\right)\right]. \end{aligned} \tag{20}$$

By substituting the terms of (18)–(20) into (17), we may arrive at the analytical OP for transmission over Rayleigh block-fading channels in the P2P-EH network in Fig. 1. If a different statistical channel model is adopted, we may reformulate (19) and (20), accordingly. Throughout this paper, we use the Rayleigh block-fading channel as a case study, although our proposed OP analysis and the search algorithms conceived for OP minimization are sufficiently general for arbitrary channel models. The effects of other wireless channel models will be investigated in our future research.

Therefore, given a specific value of L_d, the numerical evaluation of P_{out} is straightforward, according to the OP expression provided in (17). Since it relies on the single parameter L_d, a 1-D EUP-search algorithm may be designed for finding the optimal L_d, instead of searching over a 2-D EUP space, as in Section II-C. This 1D-search procedure is detailed in Algorithm 2, which is much simpler than the 2D-search algorithm in Section II-C. Specifically, in Algorithm 2, there are a total of $(L_{\max} + 1)$ candidate EUPs, since we have $L_d \in \{0, 1, \ldots, L_{\max}\}$. For each candidate EUP, the OP is evaluated using (17), where the one achieving the minimum OP is selected.

Algorithm 2 1D-Search Algorithm

```
L_{d,opt} ← 0;
P_{out,min} ← 1;
for L_d = 0 to L_max do
    P_out = P_out(L_d);
    if P_out < P_{out,min} then
        P_{out,min} ← P_out;
        L_{d,opt} ← L_d;
    end if
end for
```

[8]The optimal choice is in the context of selecting P_d for the 1D-search algorithm, which may still result in inferior OP compared to the exhaustive search and the 2D-search algorithms.

Specifically, the 1-D EUP-search procedure of Algorithm 2 requires $(L_{\max}+1)$ evaluations of the OP, which is significantly lower than that of the 2-D EUP-search of Algorithm 1 or the exhaustive search methods. The low complexity of Algorithm 2 accrues from the fact that the EUP functions $L_t(l)$ investigated may be characterized by a single scalar L_d, as shown in (16). Therefore, the OP may be expressed as a function of a scalar L_d, rather than as a vector $\overrightarrow{L_t} \triangleq \{L_t(l)|l \in [0, L_{\max}]\}$. In Section IV-A, we will compare the OP of the proposed 2D-search and 1D-search Algorithms 1 and 2 to a pair of state-of-the-art EUPs found in the literature, namely, to the best-effort policy [6] and to the asymptotic optimal policy [7].

III. Spatial-Division Multiple-Access–Energy Harvesting Network Design

In the previous section, the EUPs conceived for minimizing the OP of P2P networks were investigated. Here, we continue by investigating the EUP design of an SDMA prototype network. Compared to the P2P network, the outage events of different EH-SNs are correlated, but a centralized optimization would impose an excessive complexity. Even if a suboptimal 1-D EUP search space is adopted for each EH-SN, an M-dimensional search space is required for an SDMA network of M EH-SNs, which is generally not practical. In addition, the global knowledge of the channel quality between each EH-SN and the DN, as well as the statistical distribution of the energy arrival rates, should be available at a central controller node, which also imposes a high side-information signaling overhead and complexity. Furthermore, for traditional non-EH SDMA networks, the closed-form OP expressions are not available in the open literature for generalized SDMA networks having M SNs, since the derivation of the closed-form OP expressions for SDMA-EH networks is quite challenging.

Therefore, we embark on the OP analysis of an SDMA network relying on ML detection and use the minimum-SNR (min-SNR) approximations to arrive at the approximate OP of our SDMA networks, which has been documented in [20] and [21]. It will be shown that the min-SNR approximations are accurate in predicting the OP of the SDMA networks. Given an SDMA network comprised of M EH-SNs and a DN, we decompose the approximate joint OP of SDMA into a product of M mutually independent OP components, each of which corresponds to a P2P-EH-network counterpart. Then, we propose a DEUPO protocol, in which each EH-SN is capable of optimizing its own EUP based on the 2-D and 1-D EUP-search algorithms in Section II, using the statistics of its own uplink (UL) channel and its own energy arrival rates, indicating that only local knowledge is required.

A. System Model and OP Formulation

We consider a network of $(M+1)$ nodes, where M SNs $\{S_m, 1 \le m \le M\}$ transmit their individual information to a common DN, and each SN is equipped with both a harvesting scheme and an EB, as shown in Fig. 1. Again, we assume a narrow-band Rayleigh block-fading channel model, where the fading coefficients remain constant for the duration of a packet and then are faded independently from one packet to another in both time and space. The additive noise imposed by the receivers is modeled by independent zero-mean circularly symmetric complex Gaussian random variables with a variance of unity.

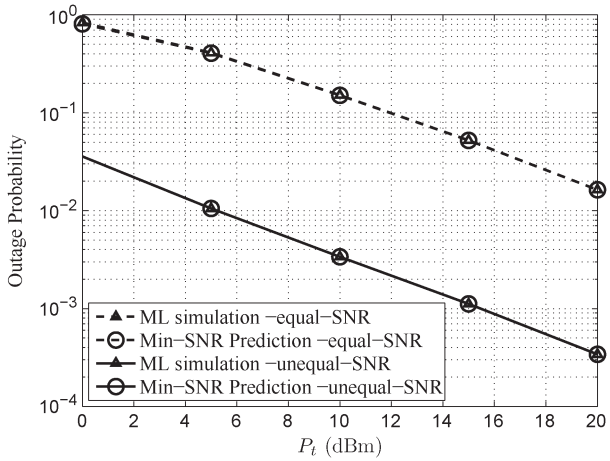

Fig. 3. Accuracy of the OP (P_{out}) evaluation using the min-SNR approximations for $M = 4$, $R = 0.5$ b/s/Hz. The distance between the SNs and the DN is $d_{sd} = 100$ m and the pathloss exponent is $\beta = 3$.

The DN is assumed to have perfect channel knowledge and adopts ML detection. All the SNs transmit their messages concurrently at the rate of R. The SN S_m encodes a bit sequence into a codeword and transmits it to the DN, where the DN jointly decodes the codewords received from all the SNs. Therefore, the SN-DN hop may be modeled by a multiple-access channel (MAC), and the criterion used for successful decoding is

$$\sum_{m\in S} R \le \log\left(1+\sum_{m\in S}\gamma_{md}\right) \ \forall S \subseteq \{S_m, 1 \le m \le M\} \tag{21}$$

where γ_{md} represents the instantaneous received SNR of the S_m-DN link. There are $(M!-1)$ inequalities in (21), and even if a single one of the inequalities in (21) is not satisfied, the transmission over the SN-DN hop becomes erroneous. Hence, when the min-SNR of the M channels spanning from the SNs to the reference node (RN), defined as $\gamma_{sd}^{\min} = \min_{m\in S}\gamma_{md}$, is lower than the threshold $\gamma_{\text{th}}^{sd} = 2^R - 1$ to be exceeded for successful decoding, an outage event occurs. Therefore, we aim for modeling the OP of the M-user MAC on the SN-RN hop with the aid of the specific SN-RN link having the min-SNR $\gamma_{sd}^{\min}$.

Specifically, in Fig. 3, we compare the OP of the M-user MAC channel using ML detection to that of a single link having the min-SNR $\gamma_{sd}^{\min}$ of the M-user system. As shown in Fig. 3, the OP of the two systems obtained by simulation perfectly matches for both the equal-SNR and the unequal-SNR scenarios. Specifically, in the equal-SNR situation, the average channel quality of the link spanning from each SN to the DN is identical, while in the unequal-SNR scenario, the average channel quality is different, where the SNRs of the $M = 4$ links are one, two, four, and eight times higher than that in the

equal-SNR situation, respectively. It is shown in Fig. 3 that the exact OP of the M-user MAC channel and the predicted OP using the P2P channel associated with the min-SNR are identical for both scenarios. Hence, the OP using the min-SNR approximation may be expressed as follows:

$$P_{\text{out},SD} \approx \Pr\left\{\min_{m\in S}\gamma_{md} < \gamma_{\text{th}}^{sd}\right\} = 1 - \Pr\left\{\min_{m\in S}\gamma_{md} \geq \gamma_{\text{th}}^{sd}\right\} = 1 - \prod_{m\in S}\Pr\left\{\gamma_{md} < \gamma_{\text{th}}^{sd}\right\} \triangleq 1 - \prod_{m\in S}(1 - P_{\text{out},md}). \tag{22}$$

B. DEUPO Protocol

Having confirmed the accuracy of the min-SNR approximation, we are now in the position to formulate the OP minimization problem for the SDMA-EH network as follows:

$$\min_{L_{t,1}(l),L_{t,2}(l),\ldots,L_{t,m}(l)} P_{\text{out},SD}\left(L_{t,1}(l), L_{t,2}(l), \ldots, L_{t,m}(l)\right) \tag{23}$$

where $L_{t,1}(l), L_{t,2}(l), \ldots, L_{t,m}(l)$ corresponds to the discrete EUPs at the SNs. Equivalently, the minimization problem defined in (23) may be expressed by

$$\max_{L_{t,1}(l),L_{t,2}(l),\ldots,L_{t,m}(l)} [1 - P_{\text{out},SD}(L_{t,1}(l), L_{t,2}(l), \ldots, L_{t,m}(l))]. \tag{24}$$

Let us now investigate the formulation of $[1 - P_{\text{out},SD}(L_{t,1}(l), L_{t,2}(l), \ldots, L_{t,m}(l))]$ in detail. By using the min-SNR approximation of (22), we have

$$[1 - P_{\text{out},SD}\left(L_{t,1}(l), L_{t,2}(l), \ldots, L_{t,m}(l)\right)] \approx \prod_{m\in S}\left[1 - P_{\text{out},md}\left(L_{t,m}(l)\right)\right]. \tag{25}$$

In order to maximize the OF of (24), we may maximize each component of $[1 - P_{\text{out},md}(L_{t,m}(l))]$. Since they are mutually independent or equivalently, we may minimize each component's $P_{\text{out},md}(L_{t,m}(l))$. This is beneficial, because the mth component $P_{\text{out},md}(L_{t,m}(l))$ corresponds to the OP of a P2P-EH link spanning from the mth EH-SN to the DN, while it is independent of both the channel quality and the EUPs adopted by other EH-SNs.

Therefore, we may design a DEUPO protocol, in which each EH-SN optimizes its own EUP relying on the proposed 1D-search and 2D-search algorithms proposed for a P2P link in Section II. Specifically, we design the protocol as follows.

- **Acquiring the Energy Arrival Rate and Channel Statistics**: In practical applications, the system designer may choose appropriate EHI and CSI estimation algorithms, through which the system may detect the changes, generate a trigger, and decide when to activate its EUP optimization. This is a widely used event-triggered protocol [22], [23]. A simpler solution is to periodically invoke the EUP optimization, according to the instantaneous estimated statistics of both the energy arrival rates and the channels. This is, however, beyond the scope of this paper. Instead, we focus our attention on the issue of deciding the EUP, whenever the optimization is activated. In our analysis, we assume that both the estimated energy arrival rate and the channel statistics are perfectly estimated. Hence, each EH-SN has perfect knowledge of the statistics of energy arrival rate, while the DN has the knowledge of the statistics of the UL channels spanning from each EH-SN. In practice, this knowledge is acquired with the aid of pilot-based channel estimation mechanism and/or prediction methods.
- **Local EUP Optimization Phase**: Each SN sends a request-to-send (RTS) packet to the DN. The DN would send M clear-to-send (CTS) packets to the M SNs, where the channel statistics between the mth EH-SN and the DN would be conveyed in each CTS packet, which is assumed to be perfectly recovered at the EH-SNs. Then, each EH-SN may adopt the 2D-search in Section II-C or the 1D-search in Section II-D to find the approximate EUP for our P2P-EH network. As discussed in the context of (25), our design objective is to minimize the approximate OP of the SDMA-EH network considered.
- **Data Transmission Phase**: Each EH-SN commences its session, by transmitting to the DN, by relying on its locally optimized EUP.

IV. Numerical Results

A. P2P Networks

As detailed in Sections II-C and D, the OP relies on the following system parameters:

- **Statistics of the energy arrival rates**: include the average energy arrival rate $\bar{P}_{\text{in}}$ and the recharge cycle T_E. The distribution of the fading energy arrival directly affects its rate, which is assumed to be exponentially distributed, as in [6] and [7], to facilitate our comparisons with the state-of-the-art benchmarkers proposed in these references.
- **Statistics of the wireless information-transfer channels**: again, the wireless channel spanning from the SN to the DN is assumed to obey Rayleigh block fading, although our analysis technique can be applied to arbitrary channel models.
- **Parameters of the EH-SN**: the EB size $B_{\max}$ and the data transmission rate R.

Here, the dependence of the OP on the aforementioned system parameters will be investigated. In the context of the P2P-EH networks, the distance between the SN and the DN is set to $d_{sd} = 100$ m and the pathloss exponent to $\beta = 3$, while the noise power at the receiver is assumed to be $N_0 = -80$ dBm. The data transmission rate is set to $R = 1$ b/s/Hz. In the figures, the analytical results are represented by the dashed curves, while the simulation results are shown by the symbols. It should be noted that the discrete step sizes ε_P used for quantifying the OP and for searching for the feasible EUP sets are different. For OP evaluations, ε_P is set for ensuring that we have $L_{\max} = 6400$ to guarantee a high accuracy of quantifying the OP, while we have ε_P set to $L_{\max} = 200$, when searching for the EUP using Algorithms 1 and 2 to control the search complexity.

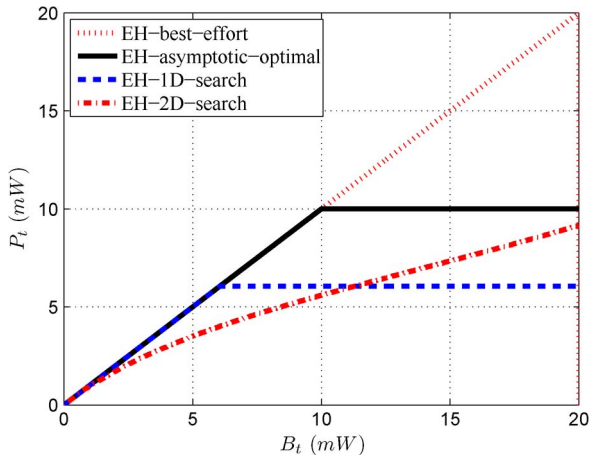

Fig. 4. Transmit power versus the EB state of different EUPs for the P2P network. The average energy arrival rate is $\bar{P}_{\rm in} = 10$ dBm, and the EB size is $B_{\max} = 16\bar{P}_{\rm in}$, while we have $R = 1$ b/s/Hz and $T_E = 8T_C$.

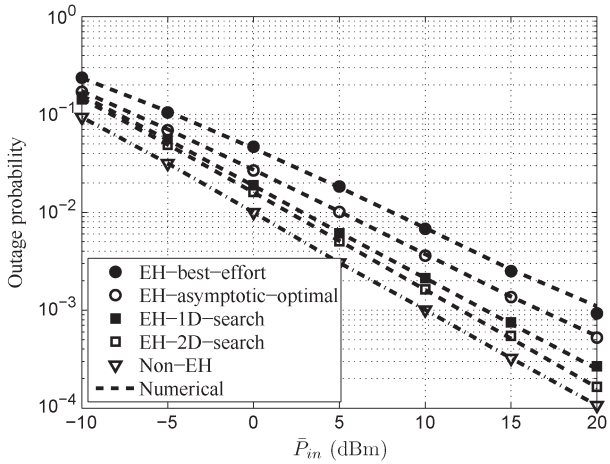

Fig. 5. OP versus average energy arrival rate $\bar{P}_{\rm in}$ using different EUPs for the P2P network. The EB size is $B_{\max} = 16\bar{P}_{\rm in}$, $R = 1$ b/s/Hz, and $T_E = 8T_C$. The numerical OP results were evaluated from (11), given the searched EUP.

We will demonstrate that the analytical results represented by the dashed curves closely match the simulation results, which indicates that the DMC-based analytical framework is capable of accurately predicting the OP of the P2P-EH networks for all of the EUPs considered.

The transmit power versus EB state of the different EUPs are characterized in Fig. 4. It is shown that the best-effort policy proposed in [6] exhibits a slope of 1, indicating that the currently harvested amount of energy in the EB will be immediately used up for transmission. The x-axis B_t represents the maximum power that may be supplied, given the amount of energy in the EB for a period of T_E. The asymptotic optimal policy is based on a combination of two trends: when the amount of energy in the EB satisfies $B_t < \bar{P}_{\rm in}$, the EH-SN transmits by employing the best-effort EUP; otherwise, its EH-SN opts for a constant power strategy by choosing a fixed transmit power of $P_t = \bar{P}_{\rm in}$. When the EB size tends to infinity, the asymptotic optimal policy would approach the performance of the constant power policy, indicating that a large EB is capable of converting an EH system into an equivalent classic non-EH system having a constant transmit power of $P_t = \bar{P}_{\rm in}$ [7]. However, when the EB size is finite, the asymptotic optimal policy is no longer optimal in terms of minimizing the OP, as shown in Fig. 5.

In Fig. 5, the performance of the EUPs found by the proposed 2D-search and 1D-search Algorithms 1 and 2 are compared to that of the best-effort policy and the asymptotic optimal policy proposed in [6] and [7], respectively. It is shown that, for the given configurations, the OP achieved by the proposed algorithms tends to be better than those achieved by the benchmarkers. Specifically, the 2D-search Algorithm 1 performs close to its classic non-EH counterpart, which serves as the lower bound of the OP for the EH systems [7]. At $P_{\rm out} = 0.01$, the EUP found by the 2D-search Algorithm 1 achieves a 3-dB power gain over the asymptotic optimal policy and a 6-dB gain over the best-effort policy. Therefore, if an EH-SN adopts the asymptotic optimal policy, it requires twice the average energy arrival rate harvested from the environment, compared with an EH-SN equipped with the proposed 2D-search algorithm, while maintaining the same OP of $P_{\rm out} = 0.01$. This ratio would, in fact, be further increased to four, if the benchmark EH-SN adopts the best-effort policy.

We may conclude that the 2D-search algorithm is capable of most significantly improving the EH-SN's capability to exploit the harvested energy, or to substantially simplify the hardware required for harvesting the energy from the environment, which is important for applications such as WSNs [1]. For example, the best-effort policy requires a four times higher average energy arrival rate for maintaining an identical outage performance as that using the 2D-search algorithm. Equivalently, the amount of power harvested by the solar panel increases linearly with the area of the solar panel [1], hence requiring a four times larger solar panel. In other words, the 2D-search Algorithm 1 allows us to design a sensor node having a solar panel of much smaller size, which has 25% of the area necessitated by the best-effort policy. Furthermore, as shown in Fig. 5, when the reliability requirements are more stringent, the performance improvements of the proposed EUPs would become more significant in terms of requiring a lower energy arrival rate or a smaller solar panel. Finally, the 1D-search Algorithm 2 is inferior to the 2D-search Algorithm 1, since it exhibits a modest performance degradation of 0.9 dB at $P_{\rm out} = 10^{-2}$. From an alternative perspective, an EH-SN adopting the 1D-search Algorithm 2 may require 1.23 times higher energy arrival rate, which is the price paid for reducing the computational complexity. Therefore, in a WSN application scenario having sensor nodes that have a low computational capability, the 1D-search Algorithm 2 or the simple asymptotic optimal policy may be preferred.

The fundamental reason for the OP improvements of the proposed 2D-search and 1D-search Algorithms 1 and 2 may be inferred from Fig. 6, which represents the PMF of the discrete EB state l for different EUPs. It is observed that all EUPs resulted in near-constant PMF values, apart from the peaks at the states, when the EB was full at $l = L_{\max}$. Compared with the PMF of the best effort and the asymptotic optimal policy, the 2D-search and 1D-search Algorithms 1 and 2 may

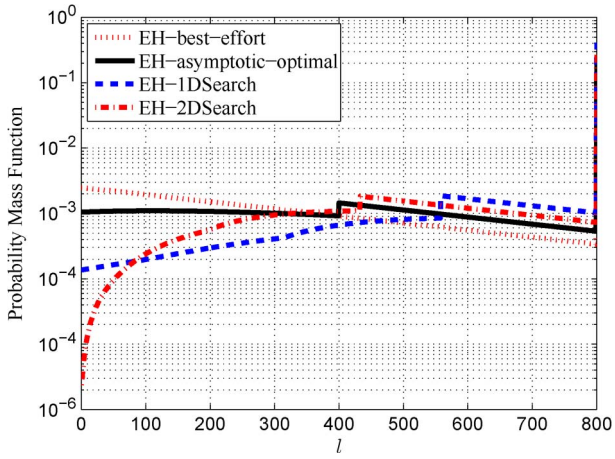

Fig. 6. PMF of the EB states for the P2P network. The average energy arrival rate is $\bar{P}_{\rm in} = 10$ dBm, while the EB size is $B_{\max} = 16\bar{P}_{\rm in}$, $R = 1$ b/s/Hz, and $T_E = 8T_C$. The results were evaluated via simulations.

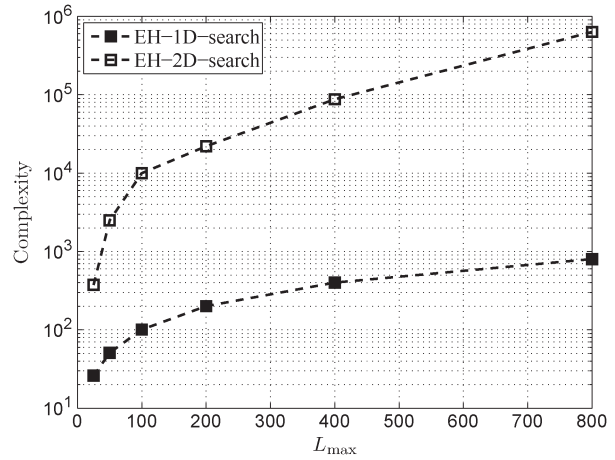

Fig. 7. Computational complexity, in terms of the number of OP evaluations versus the discrete EB size $L_{\max}$, for the 1D-search and the 2D-search algorithms for the P2P network. The results were evaluated via simulations.

be capable of improving the PMF when the EB is small, which reduces the weights π_l for the relatively large OP components of $P_e(l) = \Pr\{L_t(l)|h|^2 < L_{\rm th}\}$ in (11), when the discrete transmit power L_t is low. Therefore, reshaping the PMF by reducing the contribution of the high OP components and increasing the weights of the low OP components, the overall OP may be beneficially reduced, which is confirmed by the results in Fig. 5. It is also shown that the 1D-search Algorithm 2 may be capable of finding an EUP, which performs close to the 2D-search Algorithm 1, despite its lower complexity, as shown in Fig. 7.

More explicitly, the relationship between the number of OP evaluations and the discrete EB size $L_{\max}$ is illustrated in Fig. 7, for both the 2D-search Algorithm 1 and 1D-search Algorithm 2. Observe that the 1D-search Algorithm 2 drastically reduces the complexity of its 2D-search counterparts. Quantitatively, when the discrete EB size is $L_{\max} = 400$, the 1D-search Algorithm 2 imposes as little as 0.46% of the computational complexity compared with that of its 2D-search-based counterpart, while imposing only a modest 0.9-dB loss at $P_{\rm out} = 10^{-2}$, as shown

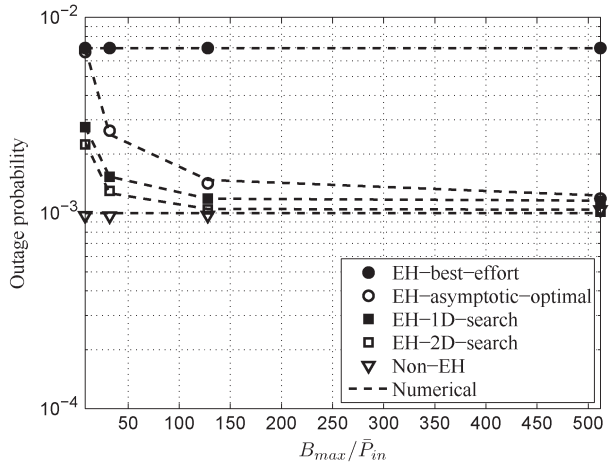

Fig. 8. OP versus the EB size $B_{\max}$ using different energy policies for the P2P network considered. The average energy arrival rate is $\bar{P}_{\rm in} = 10$ dBm, $R = 1$ b/s/Hz, and $T_E = 8T_C$. The numerical OP results were evaluated from (11), given the searched EUP.

in Fig. 5. On the other hand, from an overall energy consumption point of view, the computation of the EUP also dissipates a nonnegligible portion of the energy, particularly for users relying on low-end devices. Therefore, the 1D-search Algorithm 2 may be deemed attractive for applications relying on hardware having a low computational capability, such as mobile phones and wireless sensors.

In Fig. 8, the impact of EB size $B_{\max}$ is investigated. The horizontal axis is $B_{\max}/\bar{P}_{\rm in}$. It is shown in Fig. 8 that, when the EB size increases, the OP of both the asymptotic optimal policy proposed in [7] and the EUP relying on our 2D-search Algorithm 1 improves, and they would converge to that of their conventional non-EH counterparts. However, as the EB size $B_{\max}$ increases, the EUP found by the 2D-search Algorithm 1 may achieve a much better OP, when the EB size is small, and it may converge to that of its classic non-EH counterpart. This confirms the superiority of the proposed search algorithms conceived for EH systems having a finite EB, particularly when the available size of the EB is severely limited.

B. Multiple-Access Networks

In Fig. 9, the OP of our SDMA-EH network is investigated, and the EUPs found by the proposed 2D-search and 1D-search algorithms in Section II are compared with those of the best-effort policy and asymptotic optimal policy. It is shown that, for the given configurations, the OPs achieved by the proposed algorithms are better than those of the benchmarks. Furthermore, it is shown that the analytical results represented by dashed curves closely match the simulation results, which indicates that the proposed min-SNR approximation and the DMC-based analytical framework are accurate.

Specifically, the 2D-search algorithm performs within 2 dB from its classic non-EH counterpart at $P_{\rm out} = 10^{-2}$, which serves as the lower bound of the OP for EH systems [7]. At $P_{\rm out} = 10^{-2}$, the EUP found by the 2D-search algorithm achieves a 4.6-dB power gain compared with the asymptotic optimal policy and an 8-dB power gain compared with the

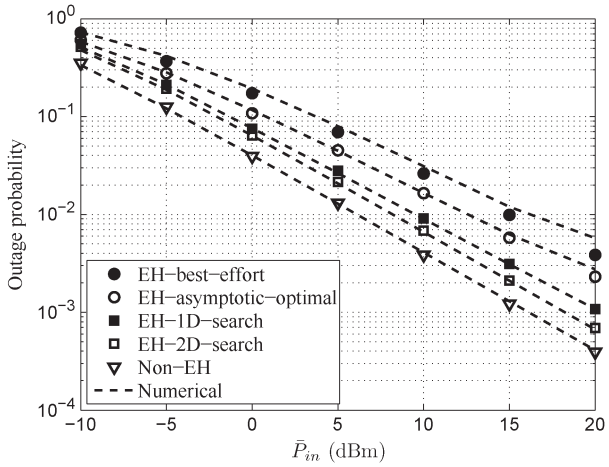

Fig. 9. OP versus average energy arrival rate $\bar{P}_{\rm in}$ using different energy policies for the SDMA network associated with $M = 4$ SNs. The EB size $B_{\max} = 16\bar{P}_{\rm in}$, $R = 1$ b/s/Hz, and $T_E = 8T_C$. The numerical OP results were evaluated from (22), given the searched EUP.

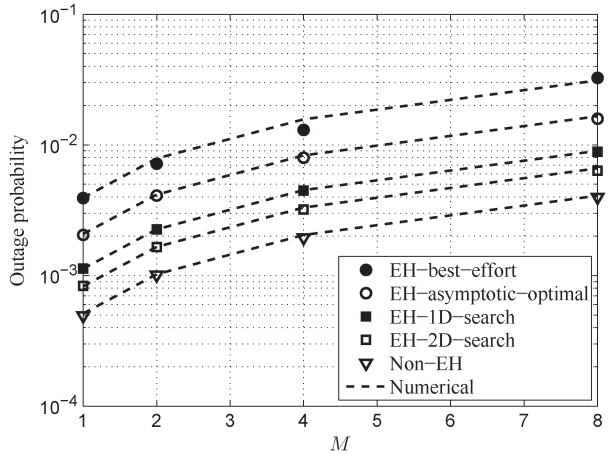

Fig. 10. OP versus average energy arrival rate $\bar{P}_{\rm in}$ using different energy policies for the SDMA network associated with different number of SNs $M = 1, 2, 4, 8$. The average energy arrival rate is $\bar{P}_{\rm in} = 10$ dBm, the EB size is $B_{\max} = 16\bar{P}_{\rm in}$, $R = 1$ b/s/Hz, and $T_E = 8T_C$. The numerical OP results were evaluated from (22), given the searched EUP.

best-effort policy. Therefore, if an EH-SN adopts the asymptotic optimal EUP, it requires $10^{4.6/10} \approx 2.9$ times higher average energy arrival rates harvested from the environment, as compared to an EH-SN equipped with the proposed 2D-search algorithm at $P_{\rm out} = 10^{-2}$. This ratio would be further increased to a factor of 6.3, if the benchmark EH-SN adopts the best-effort policy. The 1D-search algorithm is suboptimal; hence, it exhibits a performance degradation of 1.4 dB compared to that of the 2D-search algorithm at $P_{\rm out} = 10^{-3}$. From a different perspective, an EH-SN adopting our 1D-search algorithm may require a 1.4 times higher energy arrival rate, which is the price paid for its reduced computational complexity. In our future work, we will jointly consider the optimization of the energy arrival rate and of the power savings of the reduced-complexity algorithms. This might, in fact, favor the 1-D algorithm over its 2-D counterpart.

Finally, we investigate the effects of the number of EH-SNs on the OP in SDMA-EH networks. It is shown in Fig. 10 that, as the number of SNs M increases, the OP of all EUPs is reduced. However, the EUPs found by the proposed 2D-search and 1D-search algorithms always outperform both the asymptotic optimal policy and the best-effort policy. The results allow the SDMA-EH network to accommodate more users, while maintaining the same reliability. For example, if a maximum OP of $P_{\rm out} = 10^{-2}$ is tolerable in the SDMA-EH network, both the best-effort policy and the asymptotic policy may be capable of supporting $K = 2$ and 4 users, while the 1D-search and the 2D-search algorithms support more than $K = 8$ users simultaneously. To conclude, given the proposed 1D-search and 2D-search algorithms, our receiver is capable of simultaneously offering reliable services for significantly more EH users.

V. Conclusion

In this paper, we have summarized the state-of-the-art EUP design aiming for minimizing the OP of P2P-EH networks reported in the literature, and then, we have proposed two novel algorithms, which are capable of exploiting the harvested energy stored in a finite EB, where we showed that, using the proposed algorithms, the achievable OP outperforms the state-of-the-art benchmark systems found in the literature. Furthermore, upon invoking the proposed min-SNR approximation, the algorithms advocated were invoked for SDMA-EH networks, where we designed a DEUPO protocol. With the advent of the DEUPO protocols proposed in this paper, our proposed 1D- and 2D-search algorithms require a significantly reduced energy arrival rate at a given target OP.

References

[1] S. Sudevalayam and P. Kulkarni, "Energy harvesting sensor nodes: Survey and implications," *IEEE Commun. Surveys Tuts.*, vol. 13, no. 3, pp. 443–461, 3rd Quart. 2011.

[2] O. Ozel, K. Tutuncuoglu, J. Yang, S. Ulukus, and A. Yener, "Transmission with energy harvesting nodes in fading wireless channels: Optimal policies," *IEEE J. Sel. Areas Commun.*, vol. 29, no. 8, pp. 1732–1743, Sep. 2011.

[3] J. Yang and S. Ulukus, "Optimal packet scheduling in an energy harvesting communication system," *IEEE Trans. Commun.*, vol. 60, no. 8, pp. 220–230, Jan. 2012.

[4] T. Zhang *et al.*, "A cross-layer perspective on energy harvesting aided green communications over fading channels," *IEEE Trans. Veh. Technol.*, to be published. AQ5

[5] C. Huang, R. Zhang, and S. Cui, "Outage minimization in fading channels under energy harvesting constraints," in *Proc. IEEE ICC*, Jun. 2012, pp. 5788–5793.

[6] S. Luo, R. Zhang, and T. J. Lim, "Optimal save-then-transmit protocol for energy harvesting wireless transmitters," *IEEE Trans. Wireless Commun.*, vol. 12, no. 3, pp. 1196–1207, Mar. 2013.

[7] N. Zlatanov, R. Schober, and Z. Hadzi-Velkov, "Asymptotically optimal power allocation for energy harvesting communication networks," *IEEE Trans. Inf. Theory*, submitted for publication. AQ6

[8] C. Huang, R. Zhang, and S. Cui, "Optimal power allocation for outage probability minimization in fading channels with energy harvesting constraints," *IEEE Trans. Wireless Commun.*, vol. 13, no. 2, pp. 1074–1087, Feb. 2014.

[9] Y. Mao, G. Yu, and Z. Zhang, "On the optimal transmission policy in hybrid energy supply wireless communication systems," *IEEE Trans. Wireless Commun.*, vol. 13, no. 11, pp. 6422–6430, Nov. 2014.

[10] P. He, L. Zhao, S. Zhou, and Z. Niu, "Recursive waterfilling for wireless links with energy harvesting transmitters," *IEEE Trans. Veh. Technol.*, vol. 63, no. 3, pp. 1232–1241, Mar. 2014.

[11] C. K. Ho and R. Zhang, "Optimal energy allocation for wireless communications with energy harvesting constraints," *IEEE Trans. Signal Process.*, vol. 60, no. 9, pp. 4808–4818, Sep. 2012.

[12] J. Yang and S. Ulukus, "Optimal packet scheduling in a multiple access channel with energy harvesting transmitters," *J. Commun. Netw.*, vol. 14, no. 2, pp. 140–150, Apr. 2012.
[13] F. Iannello, O. Simeone, and U. Spagnolini, "Medium access control protocols for wireless sensor networks with energy harvesting," *IEEE Trans. Commun.*, vol. 60, no. 5, pp. 1381–1389, May 2012.
[14] H. Li, C. Huang, S. Cui, and J. Zhang, "Distributed opportunistic scheduling for wireless networks powered by renewable energy sources," in *Proc. IEEE Infocom*, 2014, pp. 1–9.
[15] Z. Wang, V. Aggarwal, and X. Wang, "Iterative dynamic water-filling for fading multiple-access channels with energy harvesting," pp. 1–34, Jan. 2014.
[16] D. Tse and P. Viswanath, *Fundamentals of Wireless Communication*. Cambridge, U.K.: Cambridge Univ. Press, 2005.
[17] R. Gallager, "Discrete Stochastic Processes," MIT OpenCourseWare: Massachusetts Inst. Technol., Cambridge, MA, USA, 2011.
[18] I. Krikidis, S. Timotheou, and S. Sasaki, "RF energy transfer for cooperative networks: Data relaying or energy harvesting?," *IEEE Commun. Lett.*, vol. 16, no. 11, pp. 1772–1775, Nov. 2012.
[19] V. Kulkarni, A. Forster, and G. Venayagamoorthy, "Computational intelligence in wireless sensor networks: A survey," *IEEE Commun. Surveys Tuts.*, vol. 13, no. 99, pp. 1–29, 1st Quart. 2011.
[20] B. Zhang, J. Hu, Y. Huang, M. El-Hajjar, and L. Hanzo, "Outage analysis of superposition modulation aided network coded cooperation in the presence of network coding noise," *IEEE Trans. Veh. Technol.*, vol. 64, no. 2, pp. 493–501, Feb. 2014.
[21] B. Zhang, C. Dong, J. Lei, M. El-hajjar, L.-l. Yang, and L. Hanzo, "Buffer-aided relaying for the multi-user uplink: Outage analysis and power allocation," *IEEE Trans. Veh. Technol.*, submitted for publication.
[22] C. Intanagonwiwat, R. Govindan, D. Estrin, J. Heidemann, and F. Silva, "Directed diffusion for wireless sensor networking," *IEEE/ACM Trans. Netw.*, vol. 11, no. 1, pp. 2–16, Feb. 2003.
[23] Y. Hou, H. Sherali, and S. Midkiff, "On energy provisioning and relay node placement for wireless sensor networks," *IEEE Trans. Wireless Commun.*, vol. 4, no. 5, pp. 2579–2590, Sep. 2005.

Bo Zhang received the B.Eng. degree in information engineering from the National University of Defense Technology, Changsha, China, in 2010 and the Ph.D. degree in wireless communications from the University of Southampton, Southampton, U.K., in 2015.

He is currently with the National University of Defense Technology. His research interests in wireless communications include the design and analysis of cooperative communications, multiple-input–multiple-output systems, and network-coded systems.

Chen Dong received the B.S. degree in electronic information sciences and technology from the University of Science and Technology of China, Hefei, China in 2004; the M.Eng. degree in pattern recognition and automatic equipment from the University of Chinese Academy of Sciences, Beijing, China, in 2007; and the Ph.D. degree from the University of Southampton, Southampton, U.K., in 2014.

He is a Postdoctoral Researcher with the University of Southampton His research interests include applied mathematics, relay systems, channel modelling, and cross-layer optimization.

Dr. Dong received a scholarship under the U.K.–China Scholarships for Excellence Program, and he was awarded the Best Paper Award at the Fall 2014 IEEE Vehicular Technology Conference.

Mohammed El-Hajjar received the B.Eng. degree in electrical engineering from the American University of Beirut, Beirut, Lebanon, in 2004 and the M.Sc. degree in radio frequency communication systems and the Ph.D. degree in wireless communications, both from the University of Southampton, Southampton, U.K., in 2005 and 2008, respectively.

After his Ph.D. studies, he joined Imagination Technologies as a Design Engineer, where he worked on designing and developing Imagination's multi-standard communications platform, which resulted in three patents. In January 2012, he joined the School of Electronics and Computer Science, University of Southampton, where he is a Lecturer in the Southampton Wireless Research Group. He has published a Wiley-IEEE book and more than 50 journal and international conference papers. His research interests are mainly on the development of intelligent communications systems, including energy-efficient transceiver design, cross-layer optimization for large-scale networks, multiple-input–multiple-output systems, millimeter-wave communications, and radio-over-fiber systems.

Dr. El-Hajjar has received several academic awards, including the Dean's Award for Creative Achievement, the Dorothy Hodgkin Postgraduate Award, and the 2010 IEEE International Conference on Communications Best Paper Award.

Lajos Hanzo (M'91–SM'92–F'04) received the Master's degree in electronics, the Ph.D. degree, and the Doctor Honoris Causa degree from the Technical University of Budapest, Budapest, Hungary, in 1976, 1983, and 2009, respectively, and the D.Sc. degree from the University of Southampton, Southampton, U.K., in 2004.

During his career in telecommunications, he has held various research and academic posts in Hungary, Germany, and the U.K. Since 1986, he has been with the School of Electronics and Computer Science, University of Southampton, Southampton, U.K., where he holds the Chair in telecommunications. He was a Chaired Professor with Tsinghua University, Beijing, China. He is the coauthor of 20 John Wiley/IEEE Press books on mobile radio communications, totalling in excess of 10 000 pages, and has published more than 1400 research entries on IEEE Xplore. He is currently directing an academic research team, working on a range of research projects in the field of wireless multimedia communications sponsored by industry, the Engineering and Physical Sciences Research Council (EPSRC) U.K., the European IST Program, and the Mobile Virtual Centre of Excellence, U.K. He is an enthusiastic supporter of industrial and academic liaison, and he offers a wide range of industrial courses.

Dr. Hanzo has acted as a Technical Program Committee Chair for IEEE conferences, presented keynote lectures, and has received a number of distinctions. He is the Governor of the IEEE Vehicular Technology Society and the Past Editor-in-Chief of the IEEE Press.

AUTHOR QUERIES

AUTHOR PLEASE ANSWER ALL QUERIES

AQ1 = Please check if the expanded form of RC-UK is properly captured.
AQ2 = Please check if "EH-P2P" is properly captured as "P2P-EH" to maintain consistency in the text.
AQ3 = Please check if "block Rayleigh fading channel" is properly changed to "Rayleigh block-fading channel" to maintain consistency in the text.
AQ4 = Please check if the expanded form of RN is properly captured.
AQ5 = Please provide publication update in ref. [4].
AQ6 = Please provide publication update in ref. [7].
AQ7 = Please provide title of the publication in Ref. [15].
AQ8 = Please provide publication update in ref. [21].
AQ9 = Please check if this sentence is properly inserted to maintain consistency with the current affiliation; otherwise, kindly provide changes.
AQ10 = Please check if the expanded form of FREng, FIET, and EURASIP and VTS and TPC are properly captured.

END OF ALL QUERIES

Outage Analysis and Optimization in Single- and Multiuser Wireless Energy Harvesting Networks

Bo Zhang, Chen Dong, Mohammed El-Hajjar, and Lajos Hanzo

***Abstract*—Compared to battery-powered wireless nodes having a constant but limited power supply, wireless nodes having energy harvesting (EH) capability may greatly prolong the network's sustainability. However, the energy usage policies (EUPs) have to be carefully designed according to the characteristics of the random power supply gleaned from the environment. In this paper, we carry out the outage analysis of a point-to-point (P2P) network relying on an EH transmitter, which has a finite energy buffer (EB) for transmission over a fading channel when having random energy arrival rates. A discrete Markov chain (DMC) model is proposed for characterizing the energy state of the EB, which is then used for quantifying the outage probability (OP) over the fading channels. Then, we propose both a novel 2-D and a low-complexity 1-D search algorithm for finding the specific EUPs, which are capable of minimizing the OP for the P2P network considered. It is shown that the EUP found by both algorithms outperforms the state-of-the-art EUPs disseminated in the open literature. Furthermore, we consider a multiple-access network having M EH-aided sources, where we propose a distributed EUP optimization (DEUPO) algorithm and then minimize the OP relying on the local optimization of each EH-aided source.**

***Index Terms*—Energy harvesting (EH), Markov chain, outage analysis, outage minimization.**

I. Introduction

In practical scenarios such as wireless sensor networks (WSNs), it is challenging to replace the nodes; hence, the network's operation is energy constrained, which is often formulated as having a limited lifetime [1]. One way of circumventing this problem is allowing the nodes to harvest energy from the environment. If a harvested energy source is permanently available, the transceiver can be powered perpetually, which fundamentally changes the wireless system design compared to the classic energy-constrained design relying on an energy source storing a limited amount of energy in batteries. Furthermore, based on the periodicity and magnitude of the harvested energy, the transceiver may adjust its energy usage policy (EUP) to improve certain network performance metrics, such as the throughput or outage probability (OP). The EUP may be defined as the "The policy determining the transmitting power and the transmission rate, given the availability of the knowledge on the amount of energy in the energy buffer, the channel statistic information (CSI) as well as the noncausal energy harvesting information (EHI) characterizing the energy arrival rate at the transmitter."

In this paper, we investigate both the effects of random energy arrival and of the EUP design on the OP of wireless energy harvesting (EH) networks. Recently, the EUP design of EH networks has become a hot research area. Various schemes have been proposed in the literature [2]–[9] to improve certain performance metrics in a particular network topology, relying on different assumptions of the energy arrival rates, as well as on the knowledge available at the wireless transceivers for optimization.

Under the idealized simplifying assumption of having both noncausal channel-state information (CSI) about the CSI to be encountered in the future and about the EH information (EHI) characterizing the energy arrival rate at the transmitter, in [2] and [3],[1] the optimal offline EUPs were designed for point-to-point (P2P) networks using either the throughput maximization or the file-transfer completion-time minimization as the optimization objective function (OF). Later on, the authors in [10] proposed the recursive geometric waterfilling algorithm for solving the same problem, where more efficient recursive computations were used for finding the optimal solutions. In [4], the authors modeled both the uncertainty of the energy arrival rate and that of the data arrival rate, where the transmission rate to be used was determined by minimizing the average data-buffering delay as the OF.

When the instantaneous CSI is not available at the transmitter, having an outage is unavoidable for fixed-rate applications, and the resultant OP of a P2P-EH network was investigated in [5]–[9]. The OP analysis and OP optimization techniques may be categorized into two subclasses according to the knowledge of both the energy arrival rates and the mathematical framework that they adopt; specifically, the first category of contributions recommends the employment of *time-variant policies* [5], [8], [9]. These authors followed the mathematical framework in [2]

Manuscript received December 15, 2014; revised February 19, 2015; accepted February 27, 2015. This work was supported by the Research Councils UK (RC-UK) under the auspices of the India-UK Advanced Technology Center (IU-ATC), by the European Union's Concerto Project, by the European Research Council's Advanced Fellow Grant, and by the Royal Society's Wolfson Research Merit Award. The review of this paper was coordinated by Dr. N.-D. Đào.

B. Zhang is with the School of Electronics and Electrical Engineering, National University of Defense Technology, Changsha 410073, China (e-mail: Bo.Zhang.soton@outlook.com).

C. Dong, M. El-Hajjar, and L. Hanzo are with the School of Electronics and Computer Science, University of Southampton, Southampton SO17 1BJ, U.K. (e-mail: cd2g09@ecs.soton.ac.uk; meh@ecs.soton.ac.uk; lh@ecs.soton.ac.uk).

Color versions of one or more of the figures in this paper are available online at http://ieeexplore.ieee.org.

Digital Object Identifier 10.1109/TVT.2015.2409781

[1] In [2] and [3], the terminology of "transmission policy" was used to represent the policy of using the harvested energy in the energy buffer (EB). However, the transmission policy terminology may be interpreted more widely, such as rate adaptation, multiple-access policy, etc. Therefore, to avoid ambiguity, we use the terminology of "EUP" throughout the paper.

and [11], which adopted the directional waterfilling algorithms under EH-causality constraints[2] for offline EUP design complemented by the stochastic dynamic programming in online EUP design. The time-variant policy implies the fact that the energy usage would be adapted by relying on the idealized simplifying assumptions of having the *a priori* knowledge of the instantaneous energy arrival rates. The second category of EUPs recommends *time-invariant policies for the long transmission durations* routinely encountered in WSNs, which exhibit low computational complexities [6], [7]. The terminology of a time-invariant policy reflects the fact that it does not rely on the idealized knowledge of the instantaneous energy arrival rate, regardless of whether the energy dispensation is designed according to the statistical information of the energy arrival [7] or not [6]. In this case, the EUP may be defined as the "The policy determining the transmitting power, given the amount of energy in the energy buffer and the statistical information of the channel model." *Against this backcloth, in this treatise, we aim for filling the gap between the high-complexity time-variant EUPs and the low-complexity state-of-the-art time-invariant policies, by considering scenarios having a practical finite EB*. As we will show in this paper that the EUPs in the literature [6], [7] did not exploit the EB's state and achieved a suboptimal OP performance. Hence, we propose a range of meritorious methods for improving the OP performance, which fall into the time-invariant category to impose a low computation complexity by relying merely on the knowledge of the average energy arrival rate.

As an evolution of research in the subject area of P2P-EH networks, the recent contributions on EH strategy design also cover multiple-access EH networks [6], [12]–[15]. In [12], Yang and Ulukus investigated the optimal packet scheduling problem in the context of a *two-user fading multiple-access channel*. In [15], Wang *et al.* developed optimal energy scheduling algorithms for a *generalized M-user fading multiple-access channel* relying on EH, to maximize their OF constituted by the network's sum rate, stipulating the idealized simplifying assumption that the side information of both channel states and EH states are known for a certain number of time slots (TSs), where both the battery capacity and the maximum energy consumption during each TS are finite. To the best of our knowledge, the *OP minimization problem of a generalized M-user fading multiple-access channel* is, however, an open problem. Against this background, the novel contributions of this paper are as follows.

1) An analytical framework based on a discrete Markov chain (DMC) is proposed for modeling the EB status, for the sake of investigating the OP of a P2P-EH network, in which an EH source node (EH-SN) equipped with a finite EB transmits to a destination node (DN). Given the EB's size and assuming a certain probability distribution function (PDF) for the energy arrival rate, the OP is derived for arbitrary EUPs.
2) We investigate the optimal EUP conceived for minimizing the OP of a P2P-EH network. Based on our proposed analytical framework, we show that constructing an exhaustive search for finding the optimal EUP for minimizing the OP is impractical, owing to its excessive complexity, because it scales with $(L_{\max})!$, where $L_{\max}$ is the number of states in the DMC. Therefore, a heuristic 2-D search (2D-search) algorithm is proposed for finding a meritorious EUP; we demonstrate that the proposed algorithm is potentially capable of finding the EUP at a manageable complexity.[3]
3) Nonetheless, the 2D-search algorithm conceived still exhibits a high complexity; hence, we also propose a low-complexity 1-D search (1D-search) algorithm. We will demonstrate that the OP of the 1D-search algorithm is close to that of its 2D-search counterpart, which may be attractive for applications relying on low-cost hardware, such as mobile phones and wireless sensors.
4) We extend the proposed DMC framework to more general nonorthogonal EH networks. In contrast to the P2P scenario, the outage events of practical EH-SNs tend to be correlated. As an attractive application scenario, we will investigate the OP of maximum-likelihood (ML) detection in the context of spatial-division multiple-access (SDMA) networks, we will decompose the OP by approximating it as multiple independent outage probabilities, each corresponding to a simple P2P-EH-network subproblem. Finally, we will propose a distributed EUP optimization (DEUPO) protocol, where each EH-SN is capable of optimizing its own policy using both the local statistics of the fading channel and the related energy arrival model.

The rest of this paper is organized as follows: In Section II, we first discuss the EUPs found in the literature and then invoke the DMC for modeling the EB's state. Based on this model, we consider the OP minimization problem and propose the aforementioned 2D-search and 1D-search algorithms conceived for finding the optimal EUPs. In Section III, we investigate the EUP design of SDMA-EH networks, and we propose the aforementioned distributed DEUPO protocol. Finally, our conclusions are presented in Section V.

II. Peer-To-Peer–Energy Harvesting Network Design

A. System Model and OP Formulation

We first consider a simple P2P network constituted by an SN and a DN, which is shown in Fig. 1. As shown in Fig. 1,

[2]The EH-causality constraint refers to the fact that, at any time, the transceivers can only utilize the energy that was harvested during the past and the energy not harvested as yet is hence unavailable for usage. Taking into account the causality constraints imposed on the energy usage, the energy can only be saved and used in the future. Therefore, the waterfilling algorithm is redesigned as a directional one, which allows the energy flow only to take place from the past to the future.

[3]When the Markov chain model has $L_{\max} \leq 10$ states and the number of OF evaluations is lower than 10!, the exhaustive searching may be implemented and therefore may serve as the benchmark for our proposed algorithm. However, for $L_{\max} > 10$, the complexity becomes excessive, which prevents us from verifying, whether the 2D-search algorithm is capable of matching the optimal EUP. On the other hand, it is challenging to mathematically prove the optimality of a search algorithm in the context of a nonconvex problem involving high-dimensional matrices. Therefore, this open problem will be further detailed in our discussions, and it will be investigated in our future work.

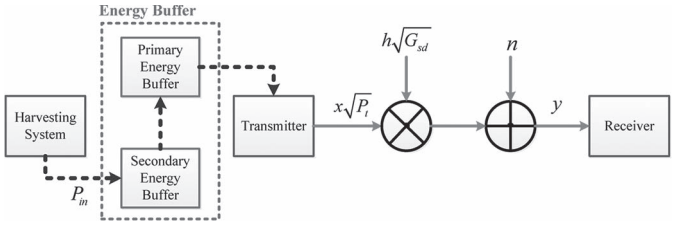

Fig. 1. System model of the P2P-EH network.

a primary EB and a secondary EB is required in practice [1], [6]. In [1], the secondary storage is a backup storage invoked for situations, when the primary storage is exhausted. In [6], the authors assumed that the rechargeable energy storage devices cannot charge and discharge simultaneously; hence, the transmitter is powered by the primary EB for data transmission, while the secondary EB is connected to the harvesting system and charges up. At the end of the recharge cycle, the secondary EB would be charged by the secondary EB. We assume that the charging time of the primary EB is negligible[4] and that the charging efficiency is assumed to be 100%.[5] Therefore, both the primary and the secondary EBs may be represented by a single EB, which is represented by the dashed-line box shown in Fig. 1. This buffer is assumed to be capable of powering the transmitter, while simultaneously being charged by the harvesting system. We do not make any specific assumptions as to what harvesting system is adopted, which may be solar cells, a wind anemometer, etc., as discussed in [1]. We assume that the EB at the SN has a finite EB size, where the harvested energy is stored and used for transmission. We assume furthermore that the energy arrival rate $P_{\rm in}$ obeys a certain probability distribution with an expectation of $\overline{P}_{\rm in}$, and it remains constant over a TS of duration T_E, while changing independently over the subsequent TSs, where a time slot is a recharge cycle. We assume that the instantaneous energy arrival rate is unknown and cannot be used during the current TS of T_E, because the secondary EB is not allowed to charge and discharge simultaneously, as shown in Fig. 1. In order to focus our attention on the EUP conceived for wireless transmission, we assume that the circuit power consumption at the SN is negligible and that the energy conversion efficiency between the EB and the transmit power is 100%.[6]

Let us now consider the channel modeling of the wireless communication links. We consider a narrow-band block-fading channel model, where the fading coefficients remain constant for the duration of a transmission packet denoted by T_C and then they are faded independently from one packet to another over the time dimension. Note that we make no assumptions concerning the specific channel model and the distribution of the channel gain. We also assume that there are always data packets buffered at the SN for transmission. The signal received at the DN is represented by

$$y = h\sqrt{P_t}G_{sd}x + n \tag{1}$$

where h is the channel coefficient capturing the effects of fading, while P_t is the transmit power, x is the transmitted signal, and n is the additive noise at the receiver, which is modeled by independent standard circularly symmetric complex Gaussian random variables having a zero mean and a variance of 1. In (1), the average processing gain of $G_{sd} = \left(N_0 \times d_{sd}^{\beta}\right)^{-1}$ between the SN and the DN captures the effect of both the pathloss and the noise, where N_0 is the noise power at the receiver, d_{sd} is the distance between the SN and the DN, while β is the pathloss exponent.

An outage is defined as the event when the instantaneous received signal-to-noise power ratio (SNR) γ at the receiver is below a predefined threshold $\gamma_{\rm th}$ that has to be exceeded for successful decoding. If idealized perfect capacity-achieving coding is assumed, we have $\gamma_{\rm th} = 2^R - 1$, where R is the data transmission rate [16]. Then, the OP of the single-hop EH network may be expressed as follows:

$$\begin{aligned} P_{\rm out} &= \Pr\left\{P_t|h|^2 G_{sd} < \gamma_{\rm th}\right\} \\ &\triangleq \Pr\left\{P_t|h|^2 < P_{\rm th}\right\} \end{aligned} \tag{2}$$

where P_t is the transmit power, and h is the normalized channel coefficient capturing the fading effects. In (2), we define $P_{\rm th} = \gamma_{\rm th}/G_{sd}$, to focus our attention on the effects of both the transmit power P_t and the channel's fading coefficient h.

In the conventional transmission scheme relying on classic constant power supply, the transmit power P_t is a constant, and the corresponding OP of narrow-band block-fading channels was quantified in [16]. However, in the EH networks, the instantaneous transmit power P_t is time variant, which is constrained by the amount of the energy available in the EB, which in turn is a random variable depending on the energy arrival rate. The energy arrival rate is assumed to exhibit a blockwise fluctuating nature, which remains constant over a TS of duration T_E and changes independently over the subsequent TSs. During a TS with a duration of T_E, the amount of energy harvested, i.e., $P_{\rm in}T_E$, is independent of both that harvested in the previous TS and of the energy consumed, i.e., P_tT_E, during transmission, which is determined by the EB state B_T at the beginning of the current TS.

We define the EB state as $B_T = B_E/T_E$, where B_E is the amount of energy available in the EB, while T_E is the duration of the recharge cycle. The physical interpretation of B_T is the maximum average transmit power that may be supported by the amount of energy stored in the buffer during the current recharge cycle.[7] *The EH-causality constraint* [2] *is interpreted*

[4]In practice, this may be realized by a supercapacitor-based storage system, such as, for example, the Everlast solar system introduced in [1].

[5]In practice, the charging efficiency of the secondary EB may not reach 100%; hence, it may be multiplied by an efficiency factor $\eta_{\rm buffer} \in [0, 1]$, which may be equivalently considered to be a reduced energy arrival rate, and hence, it does not affect any of our analysis.

[6]In practice, the power consumption of the circuits may be nonnegligible. We may assume that the harvesting system is capable of providing sufficient circuit power, while additionally providing a nonnegative transmit power. When the EH system is not capable of supplying sufficient circuit power, the transmitter may be switched off. On the other hand, the energy conversion efficiency $\eta_{\rm TX}$ from the EB to the transmitter cannot reach 100% in practice. Hence, we may simply multiply the energy arrival rate at the transmitter with an efficiency coefficient $\eta_{\rm TX} \in [0, 1]$, which does not affect any of our analysis.

[7]When the knowledge of the instantaneous CSI during a period is unavailable at the transmitter, transmitting at a constant transmit power would achieve the minimum OP [16]. Therefore, a constant transmit power is adopted during each recharge cycle, and B_T is the upper bound.

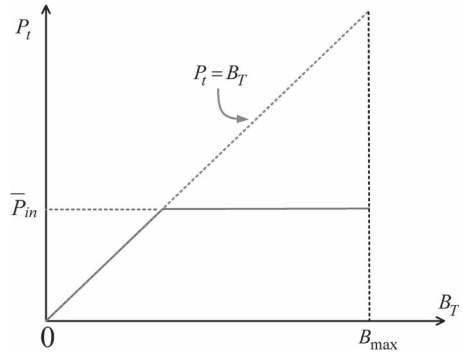

Fig. 2. EUP illustrated as the function of P_t versus B_T.

as follows: the instantaneous transmit power P_t cannot exceed the maximum power B_T that may be supported by the current EB state, i.e., we have $P_t \leq B_T$, explicitly indicating that the energy assigned for transmission must not exceed the amount of energy harvested. We may model the EUP by the transmit power as a function of the EB state, as follows:

$$P_t(B_t),\ B_T \in [0, B_{\max}] \tag{3}$$

where the EB state B_T is upper bound by $B_{\max}$ defined as the EB capacity divided by the recharge cycle T_E.

In Fig. 2, the EH-causality constraint is shown in dashed lines as $P_t(B_T) = B_T$, which models the best-effort policy proposed in [6], where all harvested energy in the buffer is used up for transmission. On the other hand, the asymptotic optimal policy proposed in [7] is illustrated by the solid line in Fig. 2, where the SN aims to transmit at a power of $P_t = \overline{P}_{\text{in}}$. In the asymptotic optimal policy, when the remaining energy in the EB is capable of supporting a higher transmit power than the average energy arrival rate $\overline{P}_{\text{in}}$, the transmitter conserves the energy for its future usage. If the remaining energy in the EB is insufficient for supporting $P_t = \overline{P}_{\text{in}}$, the SN switches to the best-effort policy. We may formulate the OP of the P2P-EH network as follows:

$$\begin{aligned} P_{\text{out}}(P_t) &= \int_0^{B_{\max}} \Pr\left\{P_t(x)|h|^2 < P_{\text{th}}\right\} f_{B_T}(x)dx \\ &= \int_0^{B_{\max}} \int_0^{+\infty} \Pr\left\{P_t(x)y < P_{\text{th}}\right\} f_{|h|^2}(y) f_{B_T}(x)dx \end{aligned} \tag{4}$$

where h is the channel coefficient capturing the effects of fading, which is a random variable, and its PDF $f_{|h|^2}(y)$ relies on the statistical channel model. $f_{B_T}(x)$, $x \in [0, B_{\max}]$ is the PDF of the EB state B_T. Therefore, to derive the OP formulated in (4), the PDF of the EB state B_T has to be modeled, bearing in mind the specific EUP adopted. Furthermore, because both P_t and B_T are continuous variables, the number of feasible EUPs is infinite, and since different policies would result in different EB-state PDFs, finding the optimal policy for minimizing the OP in (4) may be quite challenging. Hence, we will investigate this problem in the next section.

B. DMC Modeling of the EB State

As the energy arrival rate P_{in} is assumed to be constant over a recharge cycle T_E and then changes independently over the subsequent recharge cycles, the EB state $B_T(k)$ at the end of the kth $(k \geq 1)$ recharge cycle relies only on the state of $B_T(k-1)$, on the amount of energy consumed for transmission $P_t[B_T(k)]$, as well as on the current energy arrival rate P_{in}, which obeys a certain PDF, but it is statistically independent of its previous samples. Therefore, B_T may be modeled by a continuous Markov process.

However, the domain of $B_T \in [0, B_{\max}]$ is continuous; hence, the set of the states is uncountable and challenging to manage [17]. Therefore, given the EUP, deriving the PDF of B_T is quite challenging, except for certain special cases, such as the best-effort policy combined with the condition, when the transmit power is equal to the instantaneous arriving energy, which may be modeled by the exponential distribution [6]. Even for the asymptotic optimal policy [7], where P_t is a simple function determined by a combination of the best-effort policy and of the constant power supply, the PDF of B_T cannot be readily derived in closed form; hence, the asymptotic optimality relies on the fact that the probability of $\Pr\{B_T < P_t = \overline{P}_{\text{in}}\} \to 0$, when the EB size obeys $B_{\max} \to \infty$. In order to quantify and then to minimize the OP in (4), we approximate the continuous-state Markov process by a finite-state Markov chain [18], to model the EB state B_T, and to derive the PDF of B_T. Specifically, the EB size $B_{\max}$ is discretized as $L_{\max} = \lfloor B_{\max}/\varepsilon_P \rfloor$, where ε_P is the discrete step size of the power. Therefore, $l = \lfloor B_T/\varepsilon_P \rfloor$ may take a value from $l \in \{0, 1, \ldots, L_{\max}\}$ and has a state-space size of $(L_{\max} + 1)$. The instantaneous EH rate P_{in} and the decoding threshold P_{th} are also discretized with a step size of ε_P as

$$\begin{aligned} L_{\text{in}} &= \left\lfloor \frac{P_{\text{in}}}{\varepsilon_P} \right\rfloor \\ L_{\text{th}} &= \left\lfloor \frac{P_{\text{th}}}{\varepsilon_P} \right\rfloor. \end{aligned} \tag{5}$$

Hence, L_{th} is a discrete constant when P_{th} is given, while l and L_{in} are discrete random variables, and their probability mass functions (PMFs) may be generated from the PDFs of B_T and P_{in} as follows:

$$\begin{aligned} \Pr\{l = x\} &= \int_{x\varepsilon_P}^{(x+1)\varepsilon_P} f_{B_T}(u)du \\ \Pr\{L_{\text{in}} = x\} &= \int_{x\varepsilon_P}^{(x+1)\varepsilon_P} f_{P_{\text{in}}}(u)du. \end{aligned} \tag{6}$$

Although the variables B_T, P_{in}, and P_t may assume any arbitrary continuous nonnegative value, the DMC may be capable of sufficiently accurately capturing the buffer's behavior, as long as the discretization step size ε_P is small enough. Finally, we may discretize the EUP formulated in (3) as

$$P_t(l) = P_t\left(\left\lfloor \frac{B_T}{\varepsilon_P} \right\rfloor\right),\ l \in \{0, 1, \ldots, L_{\max}\} \tag{7}$$

where the discrete EUP is defined as

$$L_t(l) = \left\lfloor \frac{P_t(l)}{\varepsilon_P} \right\rfloor. \tag{8}$$

Then, we may construct the state transition matrix T of the EB states, where the specific element in the ith row and jth column is given by

$$\begin{aligned} T_{i,j} &= \Pr\{l(k+1) = j \mid l(k) = i\} \\ &= \begin{cases} \Pr\{j = i + L_{\text{in}} - L_t(i)\}, & 0 \le j < L_{\max} \\ \Pr\{j \le i + L_{\text{in}} - L_t(i)\}, & j = L_{\max}. \end{cases} \end{aligned} \tag{9}$$

We arrive at the steady-state probability vector $\pi = [\pi_0\ \pi_1\ \ldots\ \pi_{L_{\max}}]^T$ using the relationship of

$$\pi = T^T \pi \tag{10}$$

where the physical interpretation of (10) is that the state probability vector π converges and remains constant. Then, we may formulate the OP as

$$\begin{aligned} P_{\text{out}}\left(L_t(l)\right) &= \sum_{l=0}^{L_{\max}} \Pr\left\{L_t(l)|h|^2 < L_{\text{th}}\right\} \pi(l) \\ &\triangleq \sum_{l=0}^{L_{\max}} P_e(l)\pi(l) \end{aligned} \tag{11}$$

which is the discrete version of (4). It should be noted that, in (11), the OP component of $P_e(l) \triangleq \Pr\{L_t(l)|h|^2 < L_{\text{th}}\}$ is not determined unambiguously by the EUP defined by $L_t(l)$, $l \in [0, L_{\max}]$, because it also relies on the statistical channel model determining the distribution of $|h|^2$. For example, if a narrow-band Rayleigh block-fading channel is assumed, then $|h|^2$ follows the exponential distribution in conjunction with the parameter of 1. In this case, the OP component $P_e(l)$ may be expressed as

$$P_e(l) = \Pr\left\{L_t(l)|h|^2 < L_{\text{th}}\right\} = 1 - e^{-\frac{L_{\text{th}}}{L_t(l)}}. \tag{12}$$

C. Two-Dimensional EUP-Search Algorithm

Given a certain EUP represented by $L_t(l)$, $l \in [0, L_{\max}]$ and a specific statistical channel model, we are now capable of quantifying the OP of a certain EUP with the aid of (7)–(11). The optimal EUP $L_t(l)$, $l \in [0, L_{\max}]$ may be formulated by using the physically meaningful OF minimizing the OP as follows:

$$\min_{L_t(l)}\ P_{\text{out}}\left[L_t(l)\right]. \tag{13}$$

However, the inverse of the mapping in (11) from the OP $P_{\text{out}}[L_t(l)]$ to the specific EUP $L_t(l)$ cannot be readily evaluated. In other words, given a certain $P_{\text{out}}[L(l)]$, it is not possible to derive the EUP $L_t(l)$ adopted. Naturally, this hinders the related inverse mapping, and hence, the closed-form derivation of the optimal EUP is not possible. Although the buffer-state transition matrix T of (9) may be readily determined, given the EUP $L_t(l)$, according to (9), the resultant steady-state probability vector $\pi = [\pi_0\ \pi_1\ \ldots\ \pi_{L_{\max}}]^T$ is a solution of (10), which is a high-dimensional system of linear equations. Furthermore, given a certain steady-state probability vector π, it is not possible to derive the buffer-state transition matrix T, and hence, we cannot uniquely and unambiguously determine the discrete EUP $L_t(l)$.

1) Design Motivations: When using a discrete Markov modeling of the EB state, the EUP is represented by a vector of $L_t(l)$, $l \in [0, L_{\max}]$, which has $(L_{\max}+1)$ legitimate elements over the first dimension constituted by the EB state, where the lth element in $L_t(l)$ itself may be assigned any discrete value spanning from 0 to l over the second dimension representing the amount of energy assigned for transmissions. Hence, the EUP search is over a 2-D space. The aforementioned fact motivates us to design an EUP-search algorithm. The most conceptually straightforward way of finding the optimal EUP $L_t(l)$, $l \in [0, L_{\max}]$ is to invoke an exhaustive search, which evaluates every feasible EUP and selects the one having the minimum OP. As illustrated in Fig. 2, an EUP $L_t(l)$ is physically feasible as long as the instantaneous transmit power P_t is nonnegative and does not exceed the maximum affordable power B_T that may be supported by the current EB state $P_t \le B_T$, which is equivalent to the following discrete form:

$$0 \le L_t(l) \le l,\ \forall l \in [0, L_{\max}]. \tag{14}$$

This simple feasibility constraint results in a large number of feasible EUPs, where the complexity of searching for the optimal policy that minimizes the OP may be excessive. Quantitatively, there are $N_f = (L_{\max}+1)!$ number of feasible functions of $L_t(l)$, given the condition in (14). For example, if we have $L_{\max} > 11$, the number of feasible functions becomes $N_f > 10^8$. Therefore, the exhaustive search method of finding the optimal policy is not practically feasible. Hence, we have to design search algorithms having a practically tolerable complexity, which are detailed in the following sections.

2) EUP-Search Algorithm Design: In the algorithms proposed in this treatise, the design guidelines that we adopted for controlling the complexity, which is quantified by *the number of OP evaluations*, are summarized as follows.

- **Guideline 1**: *The optimal EUP $L_t(l)$, $l \in [0, L_{\max}]$ is a nondecreasing function of the EB state l, i.e., we have* $\forall k \in [0, L_{\max}-1]$, $L_t(k+1) - L_t(k) \ge 0$. The physical interpretation of this guideline can be summarized as follows. If the amount of energy available in the EB is increased, the transmitter should not use a lower transmit power. The reason behind this guideline is twofold: First, the transmitter has no knowledge of the energy arrival rate in the future; therefore; it cannot decide as to whether conserving the harvested energy in the EB for future usage is beneficial. Second, the transmitter has no knowledge of the instantaneous channel gain; therefore, it cannot decide how to control the transmit power.

- **Guideline 2**: *The increment of the optimal EUP* $L_t(l)$, $l \in [0, L_{\max}]$ *is no higher than one unit of energy with respect to the EB state* l, *i.e., we have* $\forall k \in [0, L_{\max}-1]$, $L_t(k+1) - L_t(k) \leq 1$. Let us assume that there are two feasible EUPs L_t and $\hat{L}_t$, which satisfy $L_t(k+1) - L_t(k) \geq 2$, $\hat{L}_t(k+1) - \hat{L}_t(k) \leq 1$, and $\hat{L}_t(k+1) + \hat{L}_t(k) = L_t(k+1) + L_t(k)$. When the OP versus the transmit power is a convex function, the algorithm should choose $\hat{L}_t$, because according to (11), it would achieve a lower OP than L_t, provided that the steady-state probability vector π is assumed to be fixed. However, it was shown in [8] that the OP functions with respect to the transmit power are nonconvex in the low transmit power region, i.e., when $P_{\text{out}} > 0.1$. However, in most practical scenarios, a better OP is required, in which case the OP functions tend to be convex. In this scenario, evenly allocating the transmit power to state k and $(k+1)$ may achieve a lower OP than an unequal allocation of power, given a fixed total amount of transmit power. Therefore, we judiciously opt for EUPs satisfying $L_t(k+1) - L_t(k) \leq 1$.

Although the aforementioned pair of design guidelines may be interpreted physically in a simple manner, it is challenging to rigorously prove the optimality of *Guideline 1*, while *Guideline 2* is applied in a relatively high transmit power scenario associated with a good channel quality, when the OP is a convex function of the transmit power [8]. When relying on the proposed pair of design guidelines, the number of OP evaluations is reduced from $N_f = (L_{\max})!$ to $N_{2D} = 2^{N_{\max}}$, which may still be excessive. Quantitatively, when we have $N_{\max} > 30$, the number of OF evaluations obeys $N_{2D} > 10^9$. Therefore, we conceive a third guideline for controlling the complexity, albeit this is achieved at the cost of potentially resulting in a locally optimal solution, which is detailed as follows.

- **Guideline 3**: *When the search does not find an EUP resulting in a reduced OP, it is terminated*. This is a widely used early-stopping technique employed in heuristic optimization algorithms [19]. Albeit its global optimality is not guaranteed without further information about the search space, it is capable of substantially reducing the complexity.

Since *Guideline 3* may result in locally optimal solutions, multiple initial solutions may be chosen for the search algorithm. However, through our extensive numerical evaluations conducted for $N_{\max} < 12$, when the exhaustive search algorithm is still feasible, our numerical results have shown that Algorithm 1 is capable of finding the globally optimal EUP. Algorithm 1 uses the best-effort policy as the initial solution, and then, the three aforementioned guidelines are followed throughout the rest of the design. Therefore, it may be concluded that, although the optimality may not be shown mathematically, the proposed heuristic 2D-search algorithms are effective in practical applications, while imposing a much lower complexity than the exhaustive search.

Algorithm 1 2D-Search Algorithm

$L_t(l) = l, l \in [0, L_{\max}]$;**//Start as the best-effort policy**
$P_{\text{out,min}} \leftarrow 1$;
$N_I \leftarrow 0$;
$I_U \leftarrow 1$;
while $I_U == 1$ **do**
  $N_I \leftarrow N_I + 1$; //record the number of searches
  for $l = L_{\max}$ to 0 **do**
    $\widetilde{L}_t \leftarrow L_t$; //store the current policy
    if $L_t(l) > 0$ **then**
      $L_t(l) \leftarrow L_t(l) - 1$; **//remove the top tile only (guideline 2)**.
    end if
    for $i = 0$ to l **do**
      $L_t(i) \leftarrow \min(L_t(i), L_t(l))$; **//ensure policy is non-decreasing (guideline 1)**.
    end for
    $P_{\text{out}} = P_{\text{out}}(L_t)$;
    if $P_{\text{out}} < P_{\text{out,min}}$ **then**
      $P_{\text{out,min}} \leftarrow P_{\text{out}}$;
    else
      $L_t \leftarrow \widetilde{L}_t$; //recover the stored policy
    end if
    $L_t[N_I] \leftarrow L_t$;
    if $L_t[N_I] == L_t[N_I - 1]$ **then**
      $I_U \leftarrow 0$; **//terminate if the iteration (guideline 3)**.
    end if
  end for
end while

D. One-Dimensional EUP-Search Algorithm

In the previous section, the optimal EUP was investigated and a 2D-search algorithm was proposed. However, the algorithm relies on searching in a 2-D domain of the EB state and of the energy assigned for transmission; hence, it is quite involved. Here, motivated by the fact that the asymptotic optimal policy is characterized by a constant desired transmit power [7], we formulate a 1D-search-based EUP and aim for minimizing the OP using a reduced-complexity 1-D search to exhibit a significantly lower complexity than that of the 2D-search algorithm.

1) Design Motivations: Our proposed 1D-search policy is motivated by the asymptotic optimal policy proposed in [7], which is illustrated in Fig. 2. The suboptimal EUP considered is based on a combination of the constant power policy and the best-effort policy. Specifically, given a desired constant transmit power P_d, when the energy remaining in the EB satisfies $B_t \geq P_d$, the transmitter opts for transmitting at a power of $P_t = P_d$ and conserves the rest of the energy for its future usage. Otherwise, when $B_t < P_d$, the transmitter switches to the best-effort policy and transmits at a power of $P_t = B_T$. The suboptimal policy is represented by a fixed $P_t(B_T)$ of

$$P_t(B_T) = \begin{cases} B_T, & B_T < P_d \\ P_d, & B_T \geq P_d \end{cases} \tag{15}$$

while its discrete version represented by $L_t(l), l \in [0, L_{\max}]$ is

$$L_t(l) = \begin{cases} l, & l < L_d \\ L_d, & l \geq L_d \end{cases} \tag{16}$$

where we define $L_d = \lfloor P_d/\varepsilon_P \rfloor$. Compared to the generalized representation of $L_t(l), l \in [0, L_{\max}]$, which requires $(L_{\max} + 1)$ variables for fully characterizing the policy, the proposed EUP may be characterized by a single variable L_d. Therefore, L_d is also the only variable that may be optimized to minimize the OP. However, the 1D-search policy may be expected to result in a degraded OP.

A special case of the proposed EUP is to set $P_d = \overline{P}_{\text{in}}$ or equivalently $L_d = \overline{L}_{\text{in}}$. The asymptotic optimal EUP proposed in [7] was shown to achieve the performance of its constant-power counterpart operating at $P_t = \overline{P}_{\text{in}}$, based on the assumption of an infinite EB size of $B_{\max} \to \infty$ [7]. In this case, the probability of an EB overflow is 0, and the probability of $\Pr\{B_T < P_d\} = \Pr\{l < L_d\} \to 0$. It is plausible that the performance of the classic non-EH system constitutes the OP lower bound that may be achieved by any EH system relying on a random energy arrival rate. Naturally, achieving the performance of the asymptotic optimal EUP is desirable [7].

However, when the EB size is finite, the asymptotic optimal policy would be suboptimal, because a finite EB may overflow with a nonnegligible probability, when the instantaneous energy arrival rate is high and cannot be stored for future usage. Meanwhile, the choice of $L_d = \overline{L}_{\text{in}}$ may not be optimal, since a choice of $L_d \neq \overline{L}_{\text{in}}$ may reduce both the probability of EB overflow and the OP. However, the optimal choice[8] of P_d is not obvious, because the relationship between the OP P_{out} and the energy usage function L_t is quantified by (9)–(11), which makes the direct derivation of the optimal P_d quite challenging.

By comparison, as shown in (7)–(11), given a specific value of P_d, the numerical evaluation of P_{out} may be straightforward, according to the OP expression provided in (11). This motivates us to design a search algorithm, which searches for the optimal P_d based on the numerical evaluation of P_{out}, instead of using an analytical derivation to get the optimal P_d directly.

In the next section, we will first derive the OP for the 1D-search-based EUP given a specific L_d and then propose our specific search algorithm for finding the optimal L_d to minimize the OP.

2) One-Dimensional EUP-Search Algorithm Design: Upon invoking the 1D-search-based EUP represented in (16), we may simplify the OP expression of (11) specifically for the 1D-search policy as follows:

$$\begin{aligned} P_{\text{out}} = {} & \Pr\{l \geq L_d\} \Pr\left\{L_d|h|^2 < L_{\text{th}}\right\} \\ & + \Pr\{l < L_d\} \Pr\left\{l|h|^2 < L_{\text{th}} | l < L_d\right\} \end{aligned} \tag{17}$$

where the first line represents the OP, when the energy in the EB is capable of supporting transmitting at the desired level of L_d. The second line in (17) represents the OP, when the energy in the EB is insufficient for transmitting at the power level of $L_t = L_d$, and the transmitter consumes all the energy in the EB, while transmitting at a power level of $L_t = l$. Then, we construct the state transition matrix T of the EB state according to (9), and when the EB state is steady, the state probability vector π may be formulated as follows:

$$\pi = T^T \pi$$

where $\pi = [\pi_0 \ \pi_1 \ \ldots \ \pi_{L_{\max}}]^T$. Given the desired power level represented by L_d and the OP expression in (17), we have

$$\Pr\{l \geq L_d\} = \sum_{l=L_d}^{L_{\max}} \pi_l. \tag{18}$$

If we assume furthermore that the channel obeys Rayleigh fading, the other terms in (17) can be derived as follows:

$$\Pr\left\{L_d|h|^2 < L_{\text{th}}\right\} = 1 - \exp\left(-\frac{L_{\text{th}}}{L_d}\right) \tag{19}$$

$$\begin{aligned} & \Pr\{l < L_d\} \Pr\left\{l|h|^2 < L_{\text{th}} | l < L_d\right\} \\ & = \sum_{l=0}^{L_d-1} \pi_l \Pr\left\{l|h|^2 < L_{\text{th}}\right\} \\ & = \sum_{l=0}^{L_d-1} \pi_l \left[1 - \exp\left(-\frac{L_{\text{th}}}{l}\right)\right]. \end{aligned} \tag{20}$$

By substituting the terms of (18)–(20) into (17), we may arrive at the analytical OP for transmission over Rayleigh block-fading channels in the P2P-EH network in Fig. 1. If a different statistical channel model is adopted, we may reformulate (19) and (20), accordingly. Throughout this paper, we use the Rayleigh block-fading channel as a case study, although our proposed OP analysis and the search algorithms conceived for OP minimization are sufficiently general for arbitrary channel models. The effects of other wireless channel models will be investigated in our future research. AQ3

Therefore, given a specific value of L_d, the numerical evaluation of P_{out} is straightforward, according to the OP expression provided in (17). Since it relies on the single parameter L_d, a 1-D EUP-search algorithm may be designed for finding the optimal L_d, instead of searching over a 2-D EUP space, as in Section II-C. This 1D-search procedure is detailed in Algorithm 2, which is much simpler than the 2D-search algorithm in Section II-C. Specifically, in Algorithm 2, there are a total of $(L_{\max} + 1)$ candidate EUPs, since we have $L_d \in \{0, 1, \ldots, L_{\max}\}$. For each candidate EUP, the OP is evaluated using (17), where the one achieving the minimum OP is selected.

Algorithm 2 1D-Search Algorithm

```
L_{d,opt} ← 0;
P_{out,min} ← 1;
for L_d = 0 to L_max do
    P_out = P_out(L_d);
    if P_out < P_{out,min} then
        P_{out,min} ← P_out;
        L_{d,opt} ← L_d;
    end if
end for
```

[8]The optimal choice is in the context of selecting P_d for the 1D-search algorithm, which may still result in inferior OP compared to the exhaustive search and the 2D-search algorithms.

Specifically, the 1-D EUP-search procedure of Algorithm 2 requires $(L_{\max}+1)$ evaluations of the OP, which is significantly lower than that of the 2-D EUP-search of Algorithm 1 or the exhaustive search methods. The low complexity of Algorithm 2 accrues from the fact that the EUP functions $L_t(l)$ investigated may be characterized by a single scalar L_d, as shown in (16). Therefore, the OP may be expressed as a function of a scalar L_d, rather than as a vector $\overrightarrow{L_t} \triangleq \{L_t(l)|l \in [0, L_{\max}]\}$. In Section IV-A, we will compare the OP of the proposed 2D-search and 1D-search Algorithms 1 and 2 to a pair of state-of-the-art EUPs found in the literature, namely, to the best-effort policy [6] and to the asymptotic optimal policy [7].

III. Spatial-Division Multiple-Access–Energy Harvesting Network Design

In the previous section, the EUPs conceived for minimizing the OP of P2P networks were investigated. Here, we continue by investigating the EUP design of an SDMA prototype network. Compared to the P2P network, the outage events of different EH-SNs are correlated, but a centralized optimization would impose an excessive complexity. Even if a suboptimal 1-D EUP search space is adopted for each EH-SN, an M-dimensional search space is required for an SDMA network of M EH-SNs, which is generally not practical. In addition, the global knowledge of the channel quality between each EH-SN and the DN, as well as the statistical distribution of the energy arrival rates, should be available at a central controller node, which also imposes a high side-information signaling overhead and complexity. Furthermore, for traditional non-EH SDMA networks, the closed-form OP expressions are not available in the open literature for generalized SDMA networks having M SNs, since the derivation of the closed-form OP expressions for SDMA-EH networks is quite challenging.

Therefore, we embark on the OP analysis of an SDMA network relying on ML detection and use the minimum-SNR (min-SNR) approximations to arrive at the approximate OP of our SDMA networks, which has been documented in [20] and [21]. It will be shown that the min-SNR approximations are accurate in predicting the OP of the SDMA networks. Given an SDMA network comprised of M EH-SNs and a DN, we decompose the approximate joint OP of SDMA into a product of M mutually independent OP components, each of which corresponds to a P2P-EH-network counterpart. Then, we propose a DEUPO protocol, in which each EH-SN is capable of optimizing its own EUP based on the 2-D and 1-D EUP-search algorithms in Section II, using the statistics of its own uplink (UL) channel and its own energy arrival rates, indicating that only local knowledge is required.

A. System Model and OP Formulation

We consider a network of $(M+1)$ nodes, where M SNs $\{S_m, 1 \le m \le M\}$ transmit their individual information to a common DN, and each SN is equipped with both a harvesting scheme and an EB, as shown in Fig. 1. Again, we assume a narrow-band Rayleigh block-fading channel model, where the fading coefficients remain constant for the duration of a packet and then are faded independently from one packet to another in both time and space. The additive noise imposed by the receivers is modeled by independent zero-mean circularly symmetric complex Gaussian random variables with a variance of unity.

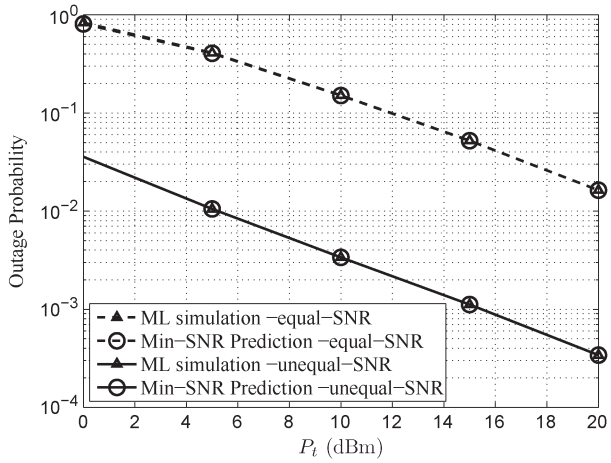

Fig. 3. Accuracy of the OP (P_{out}) evaluation using the min-SNR approximations for $M = 4$, $R = 0.5$ b/s/Hz. The distance between the SNs and the DN is $d_{sd} = 100$ m and the pathloss exponent is $\beta = 3$.

The DN is assumed to have perfect channel knowledge and adopts ML detection. All the SNs transmit their messages concurrently at the rate of R. The SN S_m encodes a bit sequence into a codeword and transmits it to the DN, where the DN jointly decodes the codewords received from all the SNs. Therefore, the SN-DN hop may be modeled by a multiple-access channel (MAC), and the criterion used for successful decoding is

$$\sum_{m\in S} R \le \log\left(1+\sum_{m\in S}\gamma_{md}\right) \ \forall S \subseteq \{S_m, 1 \le m \le M\} \tag{21}$$

where γ_{md} represents the instantaneous received SNR of the S_m-DN link. There are $(M!-1)$ inequalities in (21), and even if a single one of the inequalities in (21) is not satisfied, the transmission over the SN-DN hop becomes erroneous. Hence, when the min-SNR of the M channels spanning from the SNs to the reference node (RN), defined as $\gamma_{sd}^{\min} = \min_{m\in S}\gamma_{md}$, is lower than the threshold $\gamma_{\text{th}}^{sd} = 2^R - 1$ to be exceeded for successful decoding, an outage event occurs. Therefore, we aim for modeling the OP of the M-user MAC on the SN-RN hop with the aid of the specific SN-RN link having the min-SNR $\gamma_{sd}^{\min}$.

Specifically, in Fig. 3, we compare the OP of the M-user MAC channel using ML detection to that of a single link having the min-SNR $\gamma_{sd}^{\min}$ of the M-user system. As shown in Fig. 3, the OP of the two systems obtained by simulation perfectly matches for both the equal-SNR and the unequal-SNR scenarios. Specifically, in the equal-SNR situation, the average channel quality of the link spanning from each SN to the DN is identical, while in the unequal-SNR scenario, the average channel quality is different, where the SNRs of the $M = 4$ links are one, two, four, and eight times higher than that in the

equal-SNR situation, respectively. It is shown in Fig. 3 that the exact OP of the M-user MAC channel and the predicted OP using the P2P channel associated with the min-SNR are identical for both scenarios. Hence, the OP using the min-SNR approximation may be expressed as follows:

$$P_{\text{out},SD} \approx \Pr\left\{\min_{m\in S}\gamma_{md} < \gamma_{\text{th}}^{sd}\right\} = 1 - \Pr\left\{\min_{m\in S}\gamma_{md} \geq \gamma_{\text{th}}^{sd}\right\} = 1 - \prod_{m\in S}\Pr\left\{\gamma_{md} < \gamma_{\text{th}}^{sd}\right\} \triangleq 1 - \prod_{m\in S}(1 - P_{\text{out},md}). \tag{22}$$

B. DEUPO Protocol

Having confirmed the accuracy of the min-SNR approximation, we are now in the position to formulate the OP minimization problem for the SDMA-EH network as follows:

$$\min_{L_{t,1}(l),L_{t,2}(l),\ldots,L_{t,m}(l)} P_{\text{out},SD}\left(L_{t,1}(l), L_{t,2}(l), \ldots, L_{t,m}(l)\right) \tag{23}$$

where $L_{t,1}(l), L_{t,2}(l), \ldots, L_{t,m}(l)$ corresponds to the discrete EUPs at the SNs. Equivalently, the minimization problem defined in (23) may be expressed by

$$\max_{L_{t,1}(l),L_{t,2}(l),\ldots,L_{t,m}(l)} [1 - P_{\text{out},SD}(L_{t,1}(l), L_{t,2}(l), \ldots, L_{t,m}(l))]. \tag{24}$$

Let us now investigate the formulation of $[1 - P_{\text{out},SD}(L_{t,1}(l), L_{t,2}(l), \ldots, L_{t,m}(l))]$ in detail. By using the min-SNR approximation of (22), we have

$$[1 - P_{\text{out},SD}\left(L_{t,1}(l), L_{t,2}(l), \ldots, L_{t,m}(l)\right)] \approx \prod_{m\in S}\left[1 - P_{\text{out},md}\left(L_{t,m}(l)\right)\right]. \tag{25}$$

In order to maximize the OF of (24), we may maximize each component of $[1 - P_{\text{out},md}(L_{t,m}(l))]$. Since they are mutually independent or equivalently, we may minimize each component's $P_{\text{out},md}(L_{t,m}(l))$. This is beneficial, because the mth component $P_{\text{out},md}(L_{t,m}(l))$ corresponds to the OP of a P2P-EH link spanning from the mth EH-SN to the DN, while it is independent of both the channel quality and the EUPs adopted by other EH-SNs.

Therefore, we may design a DEUPO protocol, in which each EH-SN optimizes its own EUP relying on the proposed 1D-search and 2D-search algorithms proposed for a P2P link in Section II. Specifically, we design the protocol as follows.

- **Acquiring the Energy Arrival Rate and Channel Statistics**: In practical applications, the system designer may choose appropriate EHI and CSI estimation algorithms, through which the system may detect the changes, generate a trigger, and decide when to activate its EUP optimization. This is a widely used event-triggered protocol [22], [23]. A simpler solution is to periodically invoke the EUP optimization, according to the instantaneous estimated statistics of both the energy arrival rates and the channels. This is, however, beyond the scope of this paper. Instead, we focus our attention on the issue of deciding the EUP, whenever the optimization is activated. In our analysis, we assume that both the estimated energy arrival rate and the channel statistics are perfectly estimated. Hence, each EH-SN has perfect knowledge of the statistics of energy arrival rate, while the DN has the knowledge of the statistics of the UL channels spanning from each EH-SN. In practice, this knowledge is acquired with the aid of pilot-based channel estimation mechanism and/or prediction methods.
- **Local EUP Optimization Phase**: Each SN sends a request-to-send (RTS) packet to the DN. The DN would send M clear-to-send (CTS) packets to the M SNs, where the channel statistics between the mth EH-SN and the DN would be conveyed in each CTS packet, which is assumed to be perfectly recovered at the EH-SNs. Then, each EH-SN may adopt the 2D-search in Section II-C or the 1D-search in Section II-D to find the approximate EUP for our P2P-EH network. As discussed in the context of (25), our design objective is to minimize the approximate OP of the SDMA-EH network considered.
- **Data Transmission Phase**: Each EH-SN commences its session, by transmitting to the DN, by relying on its locally optimized EUP.

IV. Numerical Results

A. P2P Networks

As detailed in Sections II-C and D, the OP relies on the following system parameters:

- **Statistics of the energy arrival rates**: include the average energy arrival rate $\bar{P}_{\text{in}}$ and the recharge cycle T_E. The distribution of the fading energy arrival directly affects its rate, which is assumed to be exponentially distributed, as in [6] and [7], to facilitate our comparisons with the state-of-the-art benchmarkers proposed in these references.
- **Statistics of the wireless information-transfer channels**: again, the wireless channel spanning from the SN to the DN is assumed to obey Rayleigh block fading, although our analysis technique can be applied to arbitrary channel models.
- **Parameters of the EH-SN**: the EB size $B_{\max}$ and the data transmission rate R.

Here, the dependence of the OP on the aforementioned system parameters will be investigated. In the context of the P2P-EH networks, the distance between the SN and the DN is set to $d_{sd} = 100$ m and the pathloss exponent to $\beta = 3$, while the noise power at the receiver is assumed to be $N_0 = -80$ dBm. The data transmission rate is set to $R = 1$ b/s/Hz. In the figures, the analytical results are represented by the dashed curves, while the simulation results are shown by the symbols. It should be noted that the discrete step sizes ε_P used for quantifying the OP and for searching for the feasible EUP sets are different. For OP evaluations, ε_P is set for ensuring that we have $L_{\max} = 6400$ to guarantee a high accuracy of quantifying the OP, while we have ε_P set to $L_{\max} = 200$, when searching for the EUP using Algorithms 1 and 2 to control the search complexity.

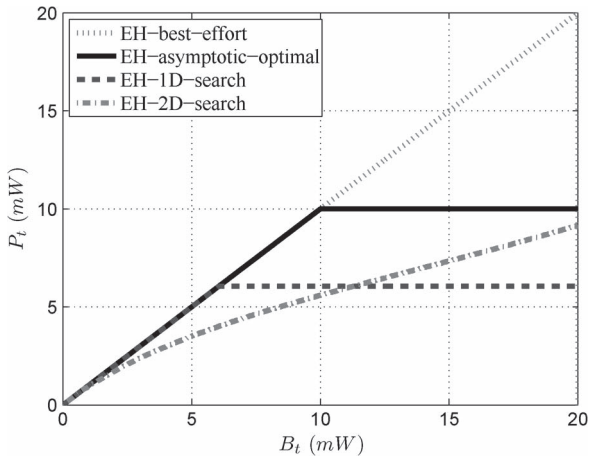

Fig. 4. Transmit power versus the EB state of different EUPs for the P2P network. The average energy arrival rate is $\bar{P}_{\rm in} = 10$ dBm, and the EB size is $B_{\max} = 16\bar{P}_{\rm in}$, while we have $R = 1$ b/s/Hz and $T_E = 8T_C$.

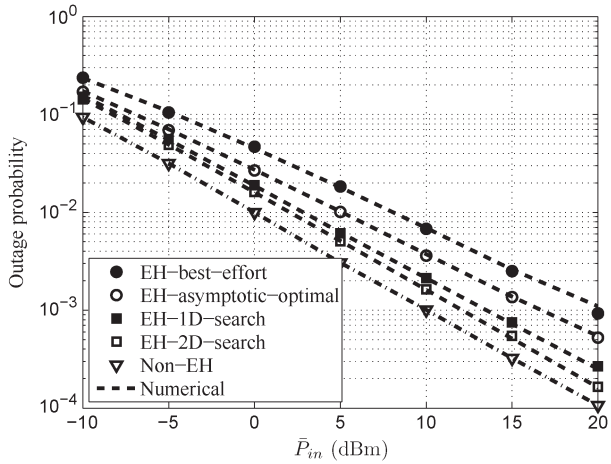

Fig. 5. OP versus average energy arrival rate $\bar{P}_{\rm in}$ using different EUPs for the P2P network. The EB size is $B_{\max} = 16\bar{P}_{\rm in}$, $R = 1$ b/s/Hz, and $T_E = 8T_C$. The numerical OP results were evaluated from (11), given the searched EUP.

We will demonstrate that the analytical results represented by the dashed curves closely match the simulation results, which indicates that the DMC-based analytical framework is capable of accurately predicting the OP of the P2P-EH networks for all of the EUPs considered.

The transmit power versus EB state of the different EUPs are characterized in Fig. 4. It is shown that the best-effort policy proposed in [6] exhibits a slope of 1, indicating that the currently harvested amount of energy in the EB will be immediately used up for transmission. The x-axis B_t represents the maximum power that may be supplied, given the amount of energy in the EB for a period of T_E. The asymptotic optimal policy is based on a combination of two trends: when the amount of energy in the EB satisfies $B_t < \bar{P}_{\rm in}$, the EH-SN transmits by employing the best-effort EUP; otherwise, its EH-SN opts for a constant power strategy by choosing a fixed transmit power of $P_t = \bar{P}_{\rm in}$. When the EB size tends to infinity, the asymptotic optimal policy would approach the performance of the constant power policy, indicating that a large EB is capable of converting an EH system into an equivalent classic non-EH system having a constant transmit power of $P_t = \bar{P}_{\rm in}$ [7]. However, when the EB size is finite, the asymptotic optimal policy is no longer optimal in terms of minimizing the OP, as shown in Fig. 5.

In Fig. 5, the performance of the EUPs found by the proposed 2D-search and 1D-search Algorithms 1 and 2 are compared to that of the best-effort policy and the asymptotic optimal policy proposed in [6] and [7], respectively. It is shown that, for the given configurations, the OP achieved by the proposed algorithms tends to be better than those achieved by the benchmarkers. Specifically, the 2D-search Algorithm 1 performs close to its classic non-EH counterpart, which serves as the lower bound of the OP for the EH systems [7]. At $P_{\rm out} = 0.01$, the EUP found by the 2D-search Algorithm 1 achieves a 3-dB power gain over the asymptotic optimal policy and a 6-dB gain over the best-effort policy. Therefore, if an EH-SN adopts the asymptotic optimal policy, it requires twice the average energy arrival rate harvested from the environment, compared with an EH-SN equipped with the proposed 2D-search algorithm, while maintaining the same OP of $P_{\rm out} = 0.01$. This ratio would, in fact, be further increased to four, if the benchmark EH-SN adopts the best-effort policy.

We may conclude that the 2D-search algorithm is capable of most significantly improving the EH-SN's capability to exploit the harvested energy, or to substantially simplify the hardware required for harvesting the energy from the environment, which is important for applications such as WSNs [1]. For example, the best-effort policy requires a four times higher average energy arrival rate for maintaining an identical outage performance as that using the 2D-search algorithm. Equivalently, the amount of power harvested by the solar panel increases linearly with the area of the solar panel [1], hence requiring a four times larger solar panel. In other words, the 2D-search Algorithm 1 allows us to design a sensor node having a solar panel of much smaller size, which has 25% of the area necessitated by the best-effort policy. Furthermore, as shown in Fig. 5, when the reliability requirements are more stringent, the performance improvements of the proposed EUPs would become more significant in terms of requiring a lower energy arrival rate or a smaller solar panel. Finally, the 1D-search Algorithm 2 is inferior to the 2D-search Algorithm 1, since it exhibits a modest performance degradation of 0.9 dB at $P_{\rm out} = 10^{-2}$. From an alternative perspective, an EH-SN adopting the 1D-search Algorithm 2 may require 1.23 times higher energy arrival rate, which is the price paid for reducing the computational complexity. Therefore, in a WSN application scenario having sensor nodes that have a low computational capability, the 1D-search Algorithm 2 or the simple asymptotic optimal policy may be preferred.

The fundamental reason for the OP improvements of the proposed 2D-search and 1D-search Algorithms 1 and 2 may be inferred from Fig. 6, which represents the PMF of the discrete EB state l for different EUPs. It is observed that all EUPs resulted in near-constant PMF values, apart from the peaks at the states, when the EB was full at $l = L_{\max}$. Compared with the PMF of the best effort and the asymptotic optimal policy, the 2D-search and 1D-search Algorithms 1 and 2 may

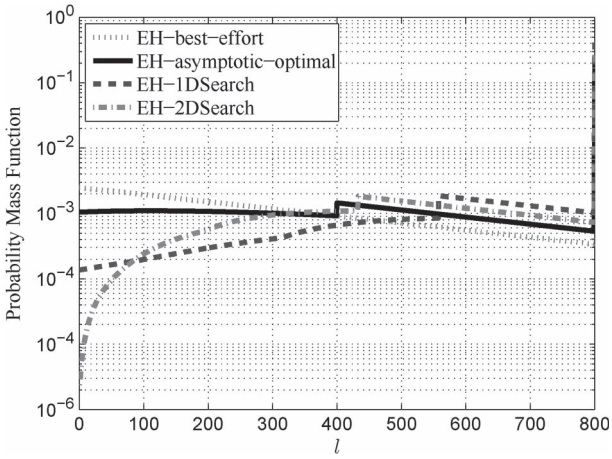

Fig. 6. PMF of the EB states for the P2P network. The average energy arrival rate is $\bar{P}_{\rm in} = 10$ dBm, while the EB size is $B_{\max} = 16\bar{P}_{\rm in}$, $R = 1$ b/s/Hz, and $T_E = 8T_C$. The results were evaluated via simulations.

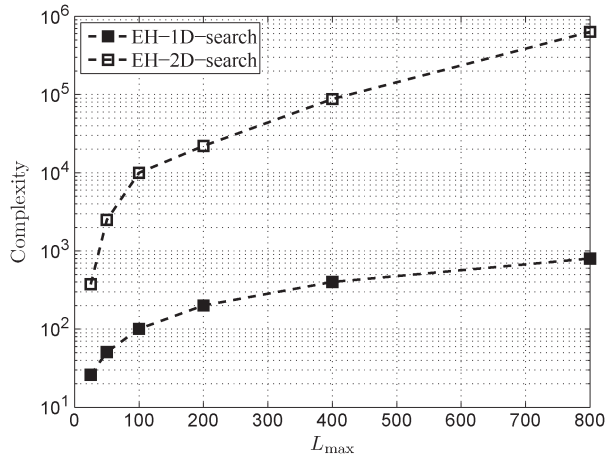

Fig. 7. Computational complexity, in terms of the number of OP evaluations versus the discrete EB size $L_{\max}$, for the 1D-search and the 2D-search algorithms for the P2P network. The results were evaluated via simulations.

be capable of improving the PMF when the EB is small, which reduces the weights π_l for the relatively large OP components of $P_e(l) = \Pr\{L_t(l)|h|^2 < L_{\rm th}\}$ in (11), when the discrete transmit power L_t is low. Therefore, reshaping the PMF by reducing the contribution of the high OP components and increasing the weights of the low OP components, the overall OP may be beneficially reduced, which is confirmed by the results in Fig. 5. It is also shown that the 1D-search Algorithm 2 may be capable of finding an EUP, which performs close to the 2D-search Algorithm 1, despite its lower complexity, as shown in Fig. 7.

More explicitly, the relationship between the number of OP evaluations and the discrete EB size $L_{\max}$ is illustrated in Fig. 7, for both the 2D-search Algorithm 1 and 1D-search Algorithm 2. Observe that the 1D-search Algorithm 2 drastically reduces the complexity of its 2D-search counterparts. Quantitatively, when the discrete EB size is $L_{\max} = 400$, the 1D-search Algorithm 2 imposes as little as 0.46% of the computational complexity compared with that of its 2D-search-based counterpart, while imposing only a modest 0.9-dB loss at $P_{\rm out} = 10^{-2}$, as shown

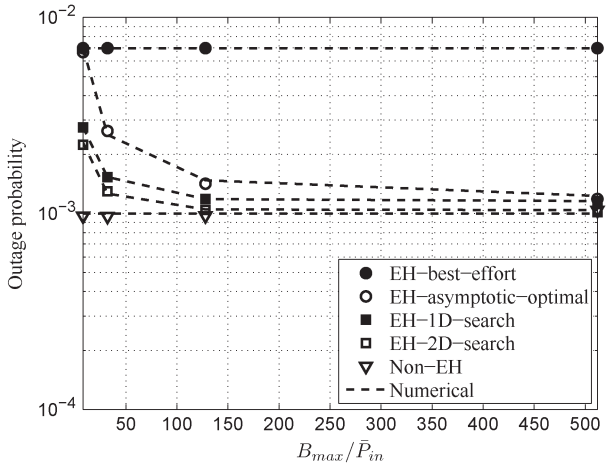

Fig. 8. OP versus the EB size $B_{\max}$ using different energy policies for the P2P network considered. The average energy arrival rate is $\bar{P}_{\rm in} = 10$ dBm, $R = 1$ b/s/Hz, and $T_E = 8T_C$. The numerical OP results were evaluated from (11), given the searched EUP.

in Fig. 5. On the other hand, from an overall energy consumption point of view, the computation of the EUP also dissipates a nonnegligible portion of the energy, particularly for users relying on low-end devices. Therefore, the 1D-search Algorithm 2 may be deemed attractive for applications relying on hardware having a low computational capability, such as mobile phones and wireless sensors.

In Fig. 8, the impact of EB size $B_{\max}$ is investigated. The horizontal axis is $B_{\max}/\bar{P}_{\rm in}$. It is shown in Fig. 8 that, when the EB size increases, the OP of both the asymptotic optimal policy proposed in [7] and the EUP relying on our 2D-search Algorithm 1 improves, and they would converge to that of their conventional non-EH counterparts. However, as the EB size $B_{\max}$ increases, the EUP found by the 2D-search Algorithm 1 may achieve a much better OP, when the EB size is small, and it may converge to that of its classic non-EH counterpart. This confirms the superiority of the proposed search algorithms conceived for EH systems having a finite EB, particularly when the available size of the EB is severely limited.

B. Multiple-Access Networks

In Fig. 9, the OP of our SDMA-EH network is investigated, and the EUPs found by the proposed 2D-search and 1D-search algorithms in Section II are compared with those of the best-effort policy and asymptotic optimal policy. It is shown that, for the given configurations, the OPs achieved by the proposed algorithms are better than those of the benchmarks. Furthermore, it is shown that the analytical results represented by dashed curves closely match the simulation results, which indicates that the proposed min-SNR approximation and the DMC-based analytical framework are accurate.

Specifically, the 2D-search algorithm performs within 2 dB from its classic non-EH counterpart at $P_{\rm out} = 10^{-2}$, which serves as the lower bound of the OP for EH systems [7]. At $P_{\rm out} = 10^{-2}$, the EUP found by the 2D-search algorithm achieves a 4.6-dB power gain compared with the asymptotic optimal policy and an 8-dB power gain compared with the

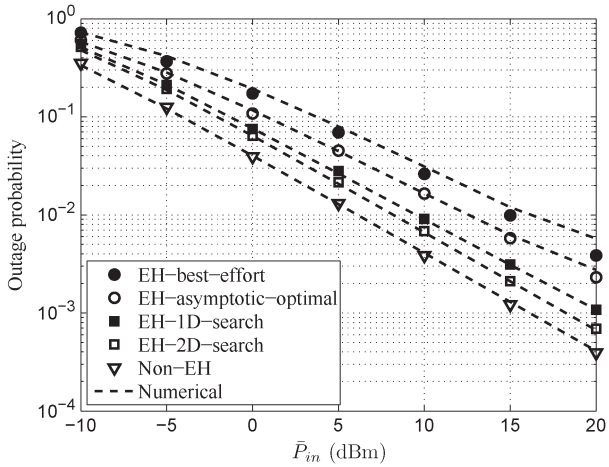

Fig. 9. OP versus average energy arrival rate $\bar{P}_{\rm in}$ using different energy policies for the SDMA network associated with $M = 4$ SNs. The EB size $B_{\max} = 16\bar{P}_{\rm in}$, $R = 1$ b/s/Hz, and $T_E = 8T_C$. The numerical OP results were evaluated from (22), given the searched EUP.

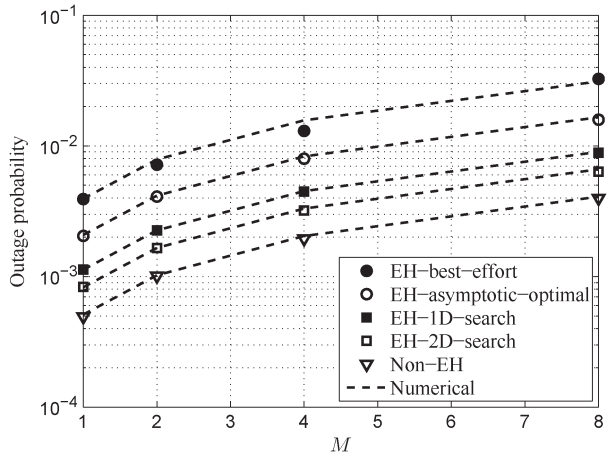

Fig. 10. OP versus average energy arrival rate $\bar{P}_{\rm in}$ using different energy policies for the SDMA network associated with different number of SNs $M = 1, 2, 4, 8$. The average energy arrival rate is $\bar{P}_{\rm in} = 10$ dBm, the EB size is $B_{\max} = 16\bar{P}_{\rm in}$, $R = 1$ b/s/Hz, and $T_E = 8T_C$. The numerical OP results were evaluated from (22), given the searched EUP.

best-effort policy. Therefore, if an EH-SN adopts the asymptotic optimal EUP, it requires $10^{4.6/10} \approx 2.9$ times higher average energy arrival rates harvested from the environment, as compared to an EH-SN equipped with the proposed 2D-search algorithm at $P_{\rm out} = 10^{-2}$. This ratio would be further increased to a factor of 6.3, if the benchmark EH-SN adopts the best-effort policy. The 1D-search algorithm is suboptimal; hence, it exhibits a performance degradation of 1.4 dB compared to that of the 2D-search algorithm at $P_{\rm out} = 10^{-3}$. From a different perspective, an EH-SN adopting our 1D-search algorithm may require a 1.4 times higher energy arrival rate, which is the price paid for its reduced computational complexity. In our future work, we will jointly consider the optimization of the energy arrival rate and of the power savings of the reduced-complexity algorithms. This might, in fact, favor the 1-D algorithm over its 2-D counterpart.

Finally, we investigate the effects of the number of EH-SNs on the OP in SDMA-EH networks. It is shown in Fig. 10 that, as the number of SNs M increases, the OP of all EUPs is reduced. However, the EUPs found by the proposed 2D-search and 1D-search algorithms always outperform both the asymptotic optimal policy and the best-effort policy. The results allow the SDMA-EH network to accommodate more users, while maintaining the same reliability. For example, if a maximum OP of $P_{\rm out} = 10^{-2}$ is tolerable in the SDMA-EH network, both the best-effort policy and the asymptotic policy may be capable of supporting $K = 2$ and 4 users, while the 1D-search and the 2D-search algorithms support more than $K = 8$ users simultaneously. To conclude, given the proposed 1D-search and 2D-search algorithms, our receiver is capable of simultaneously offering reliable services for significantly more EH users.

V. Conclusion

In this paper, we have summarized the state-of-the-art EUP design aiming for minimizing the OP of P2P-EH networks reported in the literature, and then, we have proposed two novel algorithms, which are capable of exploiting the harvested energy stored in a finite EB, where we showed that, using the proposed algorithms, the achievable OP outperforms the state-of-the-art benchmark systems found in the literature. Furthermore, upon invoking the proposed min-SNR approximation, the algorithms advocated were invoked for SDMA-EH networks, where we designed a DEUPO protocol. With the advent of the DEUPO protocols proposed in this paper, our proposed 1D- and 2D-search algorithms require a significantly reduced energy arrival rate at a given target OP.

References

[1] S. Sudevalayam and P. Kulkarni, "Energy harvesting sensor nodes: Survey and implications," *IEEE Commun. Surveys Tuts.*, vol. 13, no. 3, pp. 443–461, 3rd Quart. 2011.

[2] O. Ozel, K. Tutuncuoglu, J. Yang, S. Ulukus, and A. Yener, "Transmission with energy harvesting nodes in fading wireless channels: Optimal policies," *IEEE J. Sel. Areas Commun.*, vol. 29, no. 8, pp. 1732–1743, Sep. 2011.

[3] J. Yang and S. Ulukus, "Optimal packet scheduling in an energy harvesting communication system," *IEEE Trans. Commun.*, vol. 60, no. 8, pp. 220–230, Jan. 2012.

[4] T. Zhang *et al.*, "A cross-layer perspective on energy harvesting aided green communications over fading channels," *IEEE Trans. Veh. Technol.*, to be published. AQ5

[5] C. Huang, R. Zhang, and S. Cui, "Outage minimization in fading channels under energy harvesting constraints," in *Proc. IEEE ICC*, Jun. 2012, pp. 5788–5793.

[6] S. Luo, R. Zhang, and T. J. Lim, "Optimal save-then-transmit protocol for energy harvesting wireless transmitters," *IEEE Trans. Wireless Commun.*, vol. 12, no. 3, pp. 1196–1207, Mar. 2013.

[7] N. Zlatanov, R. Schober, and Z. Hadzi-Velkov, "Asymptotically optimal power allocation for energy harvesting communication networks," *IEEE Trans. Inf. Theory*, submitted for publication. AQ6

[8] C. Huang, R. Zhang, and S. Cui, "Optimal power allocation for outage probability minimization in fading channels with energy harvesting constraints," *IEEE Trans. Wireless Commun.*, vol. 13, no. 2, pp. 1074–1087, Feb. 2014.

[9] Y. Mao, G. Yu, and Z. Zhang, "On the optimal transmission policy in hybrid energy supply wireless communication systems," *IEEE Trans. Wireless Commun.*, vol. 13, no. 11, pp. 6422–6430, Nov. 2014.

[10] P. He, L. Zhao, S. Zhou, and Z. Niu, "Recursive waterfilling for wireless links with energy harvesting transmitters," *IEEE Trans. Veh. Technol.*, vol. 63, no. 3, pp. 1232–1241, Mar. 2014.

[11] C. K. Ho and R. Zhang, "Optimal energy allocation for wireless communications with energy harvesting constraints," *IEEE Trans. Signal Process.*, vol. 60, no. 9, pp. 4808–4818, Sep. 2012.

[12] J. Yang and S. Ulukus, "Optimal packet scheduling in a multiple access channel with energy harvesting transmitters," *J. Commun. Netw.*, vol. 14, no. 2, pp. 140–150, Apr. 2012.
[13] F. Iannello, O. Simeone, and U. Spagnolini, "Medium access control protocols for wireless sensor networks with energy harvesting," *IEEE Trans. Commun.*, vol. 60, no. 5, pp. 1381–1389, May 2012.
[14] H. Li, C. Huang, S. Cui, and J. Zhang, "Distributed opportunistic scheduling for wireless networks powered by renewable energy sources," in *Proc. IEEE Infocom*, 2014, pp. 1–9.
[15] Z. Wang, V. Aggarwal, and X. Wang, "Iterative dynamic water-filling for fading multiple-access channels with energy harvesting," pp. 1–34, Jan. 2014.
[16] D. Tse and P. Viswanath, *Fundamentals of Wireless Communication*. Cambridge, U.K.: Cambridge Univ. Press, 2005.
[17] R. Gallager, "Discrete Stochastic Processes," MIT OpenCourseWare: Massachusetts Inst. Technol., Cambridge, MA, USA, 2011.
[18] I. Krikidis, S. Timotheou, and S. Sasaki, "RF energy transfer for cooperative networks: Data relaying or energy harvesting?," *IEEE Commun. Lett.*, vol. 16, no. 11, pp. 1772–1775, Nov. 2012.
[19] V. Kulkarni, A. Forster, and G. Venayagamoorthy, "Computational intelligence in wireless sensor networks: A survey," *IEEE Commun. Surveys Tuts.*, vol. 13, no. 99, pp. 1–29, 1st Quart. 2011.
[20] B. Zhang, J. Hu, Y. Huang, M. El-Hajjar, and L. Hanzo, "Outage analysis of superposition modulation aided network coded cooperation in the presence of network coding noise," *IEEE Trans. Veh. Technol.*, vol. 64, no. 2, pp. 493–501, Feb. 2014.
[21] B. Zhang, C. Dong, J. Lei, M. El-hajjar, L.-l. Yang, and L. Hanzo, "Buffer-aided relaying for the multi-user uplink: Outage analysis and power allocation," *IEEE Trans. Veh. Technol.*, submitted for publication.
[22] C. Intanagonwiwat, R. Govindan, D. Estrin, J. Heidemann, and F. Silva, "Directed diffusion for wireless sensor networking," *IEEE/ACM Trans. Netw.*, vol. 11, no. 1, pp. 2–16, Feb. 2003.
[23] Y. Hou, H. Sherali, and S. Midkiff, "On energy provisioning and relay node placement for wireless sensor networks," *IEEE Trans. Wireless Commun.*, vol. 4, no. 5, pp. 2579–2590, Sep. 2005.

Bo Zhang received the B.Eng. degree in information engineering from the National University of Defense Technology, Changsha, China, in 2010 and the Ph.D. degree in wireless communications from the University of Southampton, Southampton, U.K., in 2015.

He is currently with the National University of Defense Technology. His research interests in wireless communications include the design and analysis of cooperative communications, multiple-input–multiple-output systems, and network-coded systems.

Chen Dong received the B.S. degree in electronic information sciences and technology from the University of Science and Technology of China, Hefei, China in 2004; the M.Eng. degree in pattern recognition and automatic equipment from the University of Chinese Academy of Sciences, Beijing, China, in 2007; and the Ph.D. degree from the University of Southampton, Southampton, U.K., in 2014.

He is a Postdoctoral Researcher with the University of Southampton His research interests include applied mathematics, relay systems, channel modelling, and cross-layer optimization.

Dr. Dong received a scholarship under the U.K.–China Scholarships for Excellence Program, and he was awarded the Best Paper Award at the Fall 2014 IEEE Vehicular Technology Conference.

Mohammed El-Hajjar received the B.Eng. degree in electrical engineering from the American University of Beirut, Beirut, Lebanon, in 2004 and the M.Sc. degree in radio frequency communication systems and the Ph.D. degree in wireless communications, both from the University of Southampton, Southampton, U.K., in 2005 and 2008, respectively.

After his Ph.D. studies, he joined Imagination Technologies as a Design Engineer, where he worked on designing and developing Imagination's multi-standard communications platform, which resulted in three patents. In January 2012, he joined the School of Electronics and Computer Science, University of Southampton, where he is a Lecturer in the Southampton Wireless Research Group. He has published a Wiley-IEEE book and more than 50 journal and international conference papers. His research interests are mainly on the development of intelligent communications systems, including energy-efficient transceiver design, cross-layer optimization for large-scale networks, multiple-input–multiple-output systems, millimeter-wave communications, and radio-over-fiber systems.

Dr. El-Hajjar has received several academic awards, including the Dean's Award for Creative Achievement, the Dorothy Hodgkin Postgraduate Award, and the 2010 IEEE International Conference on Communications Best Paper Award.

Lajos Hanzo (M'91–SM'92–F'04) received the Master's degree in electronics, the Ph.D. degree, and the Doctor Honoris Causa degree from the Technical University of Budapest, Budapest, Hungary, in 1976, 1983, and 2009, respectively, and the D.Sc. degree from the University of Southampton, Southampton, U.K., in 2004.

During his career in telecommunications, he has held various research and academic posts in Hungary, Germany, and the U.K. Since 1986, he has been with the School of Electronics and Computer Science, University of Southampton, Southampton, U.K., where he holds the Chair in telecommunications. He was a Chaired Professor with Tsinghua University, Beijing, China. He is the coauthor of 20 John Wiley/IEEE Press books on mobile radio communications, totalling in excess of 10 000 pages, and has published more than 1400 research entries on IEEE Xplore. He is currently directing an academic research team, working on a range of research projects in the field of wireless multimedia communications sponsored by industry, the Engineering and Physical Sciences Research Council (EPSRC) U.K., the European IST Program, and the Mobile Virtual Centre of Excellence, U.K. He is an enthusiastic supporter of industrial and academic liaison, and he offers a wide range of industrial courses.

Dr. Hanzo has acted as a Technical Program Committee Chair for IEEE conferences, presented keynote lectures, and has received a number of distinctions. He is the Governor of the IEEE Vehicular Technology Society and the Past Editor-in-Chief of the IEEE Press.

AUTHOR QUERIES

AUTHOR PLEASE ANSWER ALL QUERIES

AQ1 = Please check if the expanded form of RC-UK is properly captured.
AQ2 = Please check if "EH-P2P" is properly captured as "P2P-EH" to maintain consistency in the text.
AQ3 = Please check if "block Rayleigh fading channel" is properly changed to "Rayleigh block-fading channel" to maintain consistency in the text.
AQ4 = Please check if the expanded form of RN is properly captured.
AQ5 = Please provide publication update in ref. [4].
AQ6 = Please provide publication update in ref. [7].
AQ7 = Please provide title of the publication in Ref. [15].
AQ8 = Please provide publication update in ref. [21].
AQ9 = Please check if this sentence is properly inserted to maintain consistency with the current affiliation; otherwise, kindly provide changes.
AQ10 = Please check if the expanded form of FREng, FIET, and EURASIP and VTS and TPC are properly captured.

END OF ALL QUERIES